

In presenting the dissertation as a partial fulfillment of the requirements for an advanced degree from the Georgia Institute of Technology, I agree that the Library of the Institution shall make it available for inspection and circulation in accordance with its regulations governing materials of this type. I agree that permission to copy from, or to publish from, this dissertation may be granted by the professor under whose direction it was written, or, in his absence, by the Dean of the Graduate Division when such copying or publication is solely for scholarly purposes and does not involve potential financial gain. It is understood that any copying from, or publication of, this dissertation which involves potential financial gain will not be allowed without written permission.

AN INVESTIGATION OF THE SHEAR STRENGTH OF SAND AT HIGH PRESSURES

A THESIS

Presented to

The Faculty of the Graduate Division

by

Gerald Wayne Clough

In Partial Fulfillment

of the Requirements for the Degree

Master of Science in Civil Engineering

Georgia Institute of Technology

October, 1964

10/10/03

ACKNOWLEDGMENTS

The writer wishes to express his sincere appreciation to Dr. Aleksandar Sedmak Vesić for his guidance and encouragement of this investigation; and to the members of the reading committee, Professor George F. Sowers and Dr. Charles E. Weaver, for their assistance in the preparation of this manuscript.

The writer also wishes to thank all those who aided in this project by comment and discussion, particularly Professor B. B. Mazanti and Mr. Leonard Domaschuk.

Thanks are extended to Mr. C. M. Pavey for aid in solving equipment problems.

To my wife and my parents whose patience, encouragement, and assistance made this endeavor possible, I express deep gratitude.

TABLE OF CONTENTS

	Page
ACKNOWLEDGMENTS.	ii
LIST OF TABLES	v
LIST OF ILLUSTRATIONS.	vi
SUMMARY.	ix
Chapter	
I. INTRODUCTION	1
Statement of the Problem	
Review of Literature	
Purpose of the Research	
II. INSTRUMENTATION AND EQUIPMENT.	8
The Triaxial Cell	
Volume Change Devices	
The Pressure Accumulator	
Loading Machines	
Measurement of Sample Deformation	
The Membrane	
III. TESTING PROGRAM.	15
General Description of the Sand	
Preparation of Samples	
Assembly and Operation of the Testing Apparatus	
The Sieve Analysis	
The Reduction of Data	
IV. DISCUSSION OF RESULTS.	23
Reduction of Data	
Shear Strength Characteristics	
Volume Change Characteristics	
The Effect of Initial Void Ratio	
Crushing of the Grains	

	Page
V. CONCLUSIONS	43
VI. RECOMMENDATIONS FOR FURTHER STUDY	45
APPENDIX	46
BIBLIOGRAPHY	74

Westons
DEFIANCE BOND
100% COTTON FIBER

LIST OF TABLES

Table		Page
1.	Significant Properties of the Sand.	16
2.	Characteristics of the Strength Envelope for Dense Sand	28
3.	Superposition of Volume Change Components	36
4.	Summary of Initial and Final Void Ratios.	37
5.	Comparison of Initial Tangent Modulus of Elasticity to Modulus of Elasticity in Isotropic Compression	41

LIST OF ILLUSTRATIONS

Figure		Page
1.	Cross-Section of the Triaxial Cell.	10
2.	The Triaxial Cell Components.	11
3.	Triaxial Cell, Volume Change Device, and Testing Machine	11
4.	Schematic Diagram of Volume Change Device	12
5.	The Pressure Accumulator.	12
6.	Mohr Envelope and Stress Circles.	25
7.	$\frac{\sigma_1 - \sigma_3}{2}$ vs. $\frac{\sigma_1 + \sigma_3}{2}$	26
8a.	$\frac{\sigma_1 - \sigma_3}{\sigma_3}$ vs. $1/\sigma_3$	27
8b.	$\frac{\sigma_1 - \sigma_3}{\sigma_3}$ vs. $1/\sigma_3$	47
9.	Mohr Envelopes for Loose and Dense Sand at Low Pressures	48
10.	Deviator Stress, Volumetric Strain vs. Axial Strain at $\sigma_3 = 210.9$ kg. per sq. cm.	49
11.	Deviator Stress, Volumetric Strain vs. Axial Strain at $\sigma_3 = 210.9$ kg. per sq. cm.	50
12.	Deviator Stress, Volumetric Strain vs. Axial Strain at $\sigma_3 = 210.9$ kg. per sq. cm.	51
13.	Deviator Stress, Volumetric Strain vs. Axial Strain at $\sigma_3 = 632.8$ kg. per sq. cm.	52
14.	Deviator Stress, Volumetric Strain vs. Axial Strain at $\sigma_3 = 632.8$ kg. per sq. cm.	53
15.	Deviator Stress, Volumetric Strain vs. Axial Strain at $\sigma_3 = 632.8$ kg. per sq. cm.	54

Figure		Page
16.	Deviator Stress, Volumetric Strain vs. Axial Strain at $\sigma_3 = 632.8$ kg. per sq. cm.	55
17.	Deviator Stress, Volumetric Strain vs. Axial Strain at $\sigma_3 = 28.1$ and 21.1 kg. per sq. cm.	56
18.	Deviator Stress, Volumetric Strain vs. Axial Strain at $\sigma_3 = 421.8$ kg. per sq. cm.	57
19.	Volumetric Strain at Failure vs. Octahedral Normal Stress.	58
20.	Confining Pressure vs. Volumetric Strain for Tests 1, 2, 3, 7, 8	59
21.	Confining Pressure vs. Volumetric Strain for Tests 4, 5, 6, 9 and 10	60
22.	Confining Pressure vs. Volumetric Strain for Tests 11, 12, 13, 20, 21, and 22.	61
23.	Confining Pressure vs. Volumetric Strain for Tests 14, 15, 16, 17, 18, 19, 23, 24, and 25.	62
24.	Confining Pressure vs. Volumetric Strain for Tests 37 and 36	63
25.	Volume Change vs. Time After Initial Application of Confining Pressure	64
26.	Logarithm of Confining Pressure vs. Logarithm of Volumetric Strain for Tests 16 and 25	65
27.	Volumetric Strain vs. Axial Strain for Constant Octahedral Stress Tests.	66
28.	Volumetric Strain at Failure vs. Confining Pressure	67
29.	Grain Size Curves for Various Stages of Confinement	68
30.	Optical Micrograph of Original Sand Magnified 70 Times.	69
31.	Optical Micrograph of Sand Confined and Sheared at 632.8 kg. per sq. cm. Magnified 70 Times	69
32.	Grain Size Curves Contrasting Sheared Samples and Isotropically Confined Samples.	70
33.	Bulging Failure at 210.9 kg. per sq. cm.	71

Figure	Page
34. Bulging Failure at 632.8 kg. per sq. cm.	71
35. Initial Tangent Modulus of Deformation vs. Confining Pressure.	72
36. Extrapolated Sand Envelope to Meet Quartz Envelope.	73

SUMMARY

With the advent of nuclear cratering and the recognition of the significance of the very high pressures occurring under the tips of piles or under and within large earth dams, a need has arisen for increased knowledge of the behavior of soils at very high pressures. The purpose of this research was to investigate the shear strength and volume change characteristics of a sand at pressures up to 633 kg. per sq. cm.

Standard triaxial tests and constant octahedral tests were run in a high pressure triaxial cell on dry and saturated Chattahoochee River sand in both a loose and dense state, measuring shear strength and volume change. The samples were two inches in diameter and approximately five inches in height. The confining pressure was varied from about 20 kg. per sq. cm. to over 600 kg. per sq. cm. in the triaxial tests and from 1 kg. per sq. cm. to over 300 kg. per sq. cm. in the constant octahedral stress tests.

The shear strength circles indicated that the strength envelope in the pressure range exceeding 50 kg. per sq. cm. could be approximated by a straight line of a slope of about 32 degrees for both loose and dense sand. Below that pressure range, the dense envelope assumed a certain degree of curvature, varying with the confining pressure.

Explaining the curvature in the dense envelope involved conducting a series of constant octahedral shear tests to investigate the phenomenon of dilatancy. The constant octahedral shear tests isolated the volume

change due to shear and showed that the volume increase of dense sand at low pressures existed approximately over the range of pressures which contained envelope curvature. Loose samples underwent volume decrease over the whole range of pressures tested in the constant octahedral tests, whereas the dense samples increased in volume when subjected to octahedral normal stresses up to 30 kg. per sq. cm. and decreased in volume above that pressure.

Volume change measurements during application of confining pressure indicated that samples that were initially both loose and dense had achieved the same density after confinement exceeding about 180 kg. per sq. cm. The loose and dense curves for volume change during octahedral shear came together at approximately 200 kg. per sq. cm. as did the volume change curves in the case of conventional triaxial shear.

The isolated volume change components, as represented by the volumetric strain versus confining pressure and volumetric strain at failure versus octahedral stress curves, were superimposed. This superposition of the two volume-change components gave an insight to the variation of volume change with confining pressure in a conventional triaxial test in which a sample is subjected to both shear and increasing octahedral normal stresses. This indicated the possibility of prediction of volumetric strain at failure due to shear alone under a given confining pressure by subtracting the appropriate value found from the volumetric strain versus confining pressure curves from the volumetric strain under triaxial shear which occurred at that confining pressure.

Comparison of samples after testing revealed significant grain crushing at pressures as low as 20 kg. per sq. cm. It was also found

that considerably more crushing of grains took place under the action of shearing than under isotropic compression.

CHAPTER I

INTRODUCTION

Statement of the Problem

The shear strength of soils has long been a subject of extensive investigation in the field of soil mechanics. However, the shear strength research done has been largely restricted to tests wherein the soil was laterally confined by pressures not exceeding 10 kg. per sq. cm. Since the inception of the new field of explosive cratering and the recognition of high pressures associated with deep foundations and very large earth dams, a need for the investigation of the shear strength of soils at confining pressures far above those previously used has been acknowledged. The pressures associated with the phenomenon of cratering by deeply buried nuclear devices extend from thousands of kilograms per square centimeter to melting pressures (1), while those associated with the latter fields are somewhat lower, but still well above conventional pressures.

Research into the behavior of soils at high pressures has been so limited that the necessity for such an investigation is undeniable.

Review of Literature

The uniqueness of high pressure triaxial testing of soils is underscored by the fact that only one published paper exists on the subject above pressures of 40 kg. per sq. cm. High pressure triaxial testing of rock has been extensively conducted by von Kármán (2), Bridgman

(3), Griggs (4), et al., but this work was never extended to include soils. The U. S. Bureau of Reclamation pioneered high pressure tri-axial testing in connection with the design of dam foundations (5) and nuclear cratering with a device capable of applying confining pressures up to 8,800 kg. per sq. cm., but limited their work only to rock encountered in specific projects.

The effect of the large axial loads which are associated with high confining pressures has been observed by several investigators. Terzaghi and Peck (6) noted that in a laterally confined sample, the grains of a sand began to be crushed at a pressure of about 100 kg. per sq. cm. resulting in increased compressibility up to about 1,000 kg. per sq. cm.

In 1960, Ladanyi (7) observed the occurrence of crushing of quartz grains in a sand tested in a triaxial apparatus at confining pressures of 25 kg. per sq. cm.

De Beer (8), in an effort to determine the influence of grain crushing on penetration resistance, reported on two types of tests performed with different forms of confinement. The first dealt with a laterally fully confined sample loaded by a 1,000-ton press. The results generally confirmed those obtained by Terzaghi and Peck. From 0 to 150 kg. per sq. cm., the compressibility of the laterally confined sample decreases as unit pressures increase. At about 150 kg. per sq. cm., crushing of the grains begins to take place and facilitates rearrangement of the particles, thus giving rise to an increased compressibility as the unit pressure increases. When 350 kg. per sq. cm. was reached, the number of points of contact had increased sufficiently to cause a decrease

in compressibility with increased crushing. This would continue theoretically until all voids were eliminated at which point the material would be reduced to quartz, though not necessarily crystalline quartz.

The second type of test reported by De Beer was similar to the first, but more freedom of movement was allowed the particles of sand. A cylindrical piston was forced through a circular steel plate which formed the top of a rigid steel container for the sand specimen. To prevent any upheaval of the top plate, two hydraulically loaded beams were brought to bear upon the plate if any such movement were detected.

De Beer hypothesized that with the additional liberty of movement, higher shear stresses would be induced, thus causing increased crushing of grains and creating a situation which closely simulated the conditions encountered under a deep-seated loading area. To substantiate this hypothesis, De Beer presented a grain size distribution corresponding to a unit load beneath the piston in the case of the second type test of 400 kg. per sq. cm. which was much finer than one corresponding to a unit load of 450 kg. per sq. cm. from the first type of test.

This experimental data would thus account for the fact that the volume change of a sand was greater than that anticipated by formulae of pure expulsion of an incompressible material.

Hirschfield and Poulos (9) performed triaxial tests on two soil types, a silt and a sand, up to pressures of 40 kg. per sq. cm., measuring both shear strength and volume change characteristics. The silt was tested in an undisturbed condition, whereas the sand was compacted and vibrated into its densest configuration. All specimens had a diameter of 3.58 cm. and an average height of 8.5 cm.

The results of the tests indicated some curvature in the envelopes of both materials, despite the fact, as the authors note, that the coefficient of friction between quartz grains is approximately constant over a 50-fold variation of normal stress (10), suggesting a straight line envelope through the origin. Since significant volume changes occurred in the tests throughout the range of confining pressures, the authors attempted to explain at least part of the curvature through volume change-work considerations. This effect was quantitatively corrected by the authors using the "stress-dilatancy" equation derived by Rowe (10). The resulting envelope for sand was a straight line and for the silt closely approximated a straight line, the slight residual curvature being attributed to overconsolidation. The significant findings of Hirschfield and Poulos may be summarized as follows:

1. The volume of the sample decreased throughout shear at confining pressures of 40 kg. per sq. cm.
2. The initial tangent modulus of deformation increases non-linearly with confining pressure.
3. Extrapolation of shear strength data is not possible from low to high pressures.
4. Curvature of the Mohr envelope may be largely due to volume change.

Triaxial tests on sand at pressures up to 632 kg. per sq. cm. have been performed and reported by Vesić and Barksdale in 1963 (11). Seventeen samples 2.22 cm. in diameter and about 4.5 cm. in height were tested by the standard triaxial procedure in a high pressure cell with volume change measured in one test. Two samples of the same dimensions were

tested under a constant octahedral normal stress with volume change measurements being made as in the standard test by water burette.

It was found that the Mohr envelope had considerable curvature in the range of pressures from 0 to 50 kg. per sq. cm. However, beyond 50 kg. per sq. cm. the curvature disappeared. Of course, this effect was not noticed in earlier investigations since the pressures in the previous tests did not extend past 40 kg. per sq. cm.

Volume change was also assumed by Vesić and Barksdale to be the causative element in the curvature of the envelope, but the substantiation of the assumption was undertaken by a different approach from that of Hirschfield and Poulos. By means of constant octahedral normal stress tests, eliminating volume change due to hydrostatic components of stress, the volume change caused by shear alone was measured. In a test conducted at a mean normal stress of 47 kg. per sq. cm., the net volume change was approximately zero, implying that the dilatancy component of shear strength had vanished, thus eliminating curvature beyond 50 kg. per sq. cm. This would suggest that the frictional component of shear strength remained proportional to the octahedral normal stress over the entire range of pressures tested. The authors proved that above 50 kg. per sq. cm. shear was made possible by crushing and breakage of particles and that the volume change throughout shear was a decrease.

Considerable crushing of grains was found by Vesić and Barksdale at the higher chamber pressures. The authors also made comparative tests between crushing by pure compression at 632 kg. per sq. cm. and crushing by subsequent application of shearing forces at that pressure. In confirmation of the hypothesis set forth by De Beer (8), the sheared sand

had a much finer grain distribution curve than did the isotropically confined sand.

From data reported by Barksdale in an unpublished paper (12), the initial tangent modulus of deformation was found to vary approximately with the square root of the confining pressure for the sand tested. The two soils tested by Hirschfield and Poulos presented results which were in general agreement with this relationship.

This literature review constitutes the whole of the published information on soils and soil testing at high pressures. This absence of known data on an important question is one of the reasons for this study.

Purpose of the Research

This study proposes to:

1. establish the shape of the Mohr envelope for the sand used in the investigation,
2. determine the effect of initial void ratio on the shear strength and volume change characteristics,
3. examine quantitatively the phenomenon of crushing of grains during both isotropic compression and shear,
4. investigate the nature of the volume change of the sand being tested during isotropic compression, and
5. investigate the phenomenon of volume change under shear isolated from the usual accompanying volume change due to increasing mean normal stress.

The research will be performed on cohesionless Chattahoochee River

sand chosen because of its availability and a thorough knowledge of its basic properties as determined by exhaustive testing by previous investigators (13).

CHAPTER II

INSTRUMENTATION AND EQUIPMENT

The Triaxial Cell

The triaxial cell was designed to permit testing of samples up to 2 inches in diameter and approximately 5 inches in height at lateral pressures as high as 10,000 psi.

The 8 inch diameter base was constructed of bearing bronze with a yield strength of 20,000 to 24,000 psi and a Brinell Hardness of 53.3. Provisions were made for 3 pressure connections:

1. The connection for filling the cell with fluid to apply the all-round chamber pressure.
2. The connection with the base of the sample, to provide for drainage of the sample.
3. The connection with the top cap of the sample, for any future use of the cell which required two-way drainage of the specimen.

At the center of the base was a threaded hole designed to receive a high strength steel pedestal which acted as a base for the sample. Sealing this coupling was accomplished by one rubber O-ring at the bottom of the pedestal.

The cylinder which threaded onto the base was made of cold-drawn, seamless steel tubing of 55,000 psi yield strength. The cylinder had an inside diameter of 3.50 inches, a wall thickness of 13/16 inch, and a height of 12-13/16 inches. At the bottom of the cylinder the seal was

provided by one rubber O-ring contained in a groove in the cylinder. The top of the cylinder was threaded to receive the piston assembly which consisted of a bronze packing gland with a 1-1/4 inch hole in the center and the cell piston which passed through the hole. The 1-1/4 inch diameter piston was made of high strength steel with a yield strength of 130,000 psi. Between the packing gland and the cylinder the seal was accomplished by one rubber O-ring contained in a groove at the bottom of the packing gland. The movable piston in the center of the packing gland was sealed by three rubber O-rings contained in grooves inscribed in the packing gland.

A top cap of high strength steel was placed on the sample to distribute the load from the piston to the sample. A small depression was provided in the center of the top cap to receive the rounded end of the piston.

At the top of the cylinder a valve was located to allow air to escape as the confining fluid was entering the cell through the base. The cell is illustrated in Figures 1, 2 and 3.

Volume Change Devices

In the majority of the tests, the volume change was measured on dry samples by a constant pressure air system. It was connected to the sample through the pressure connection with the base of the sample. A schematic diagram of the device, constructed essentially after Bishop and Henkel (14), is shown in Figure 4.

The adjustable column of fluid in the burette was mercury, whose height was adjusted by air pressure admitted through a regulatory valve.

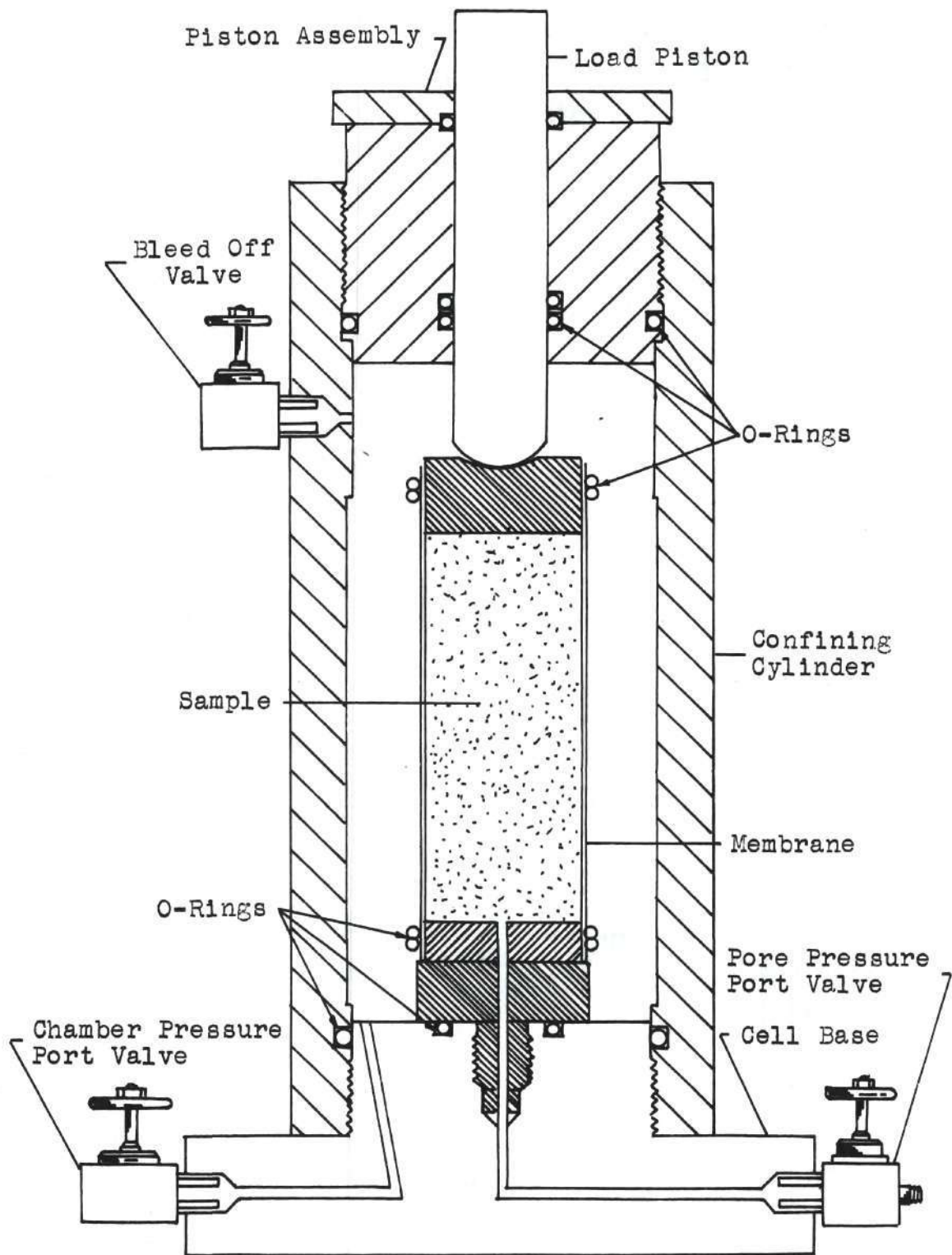


Figure 1. Cross-section of the Triaxial Cell.

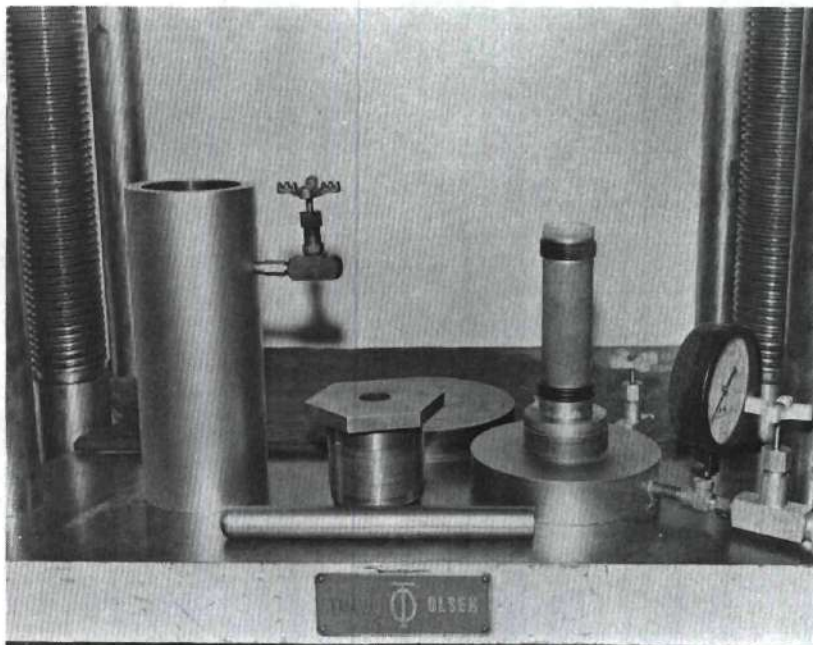


Figure 2. The Triaxial Cell Components.

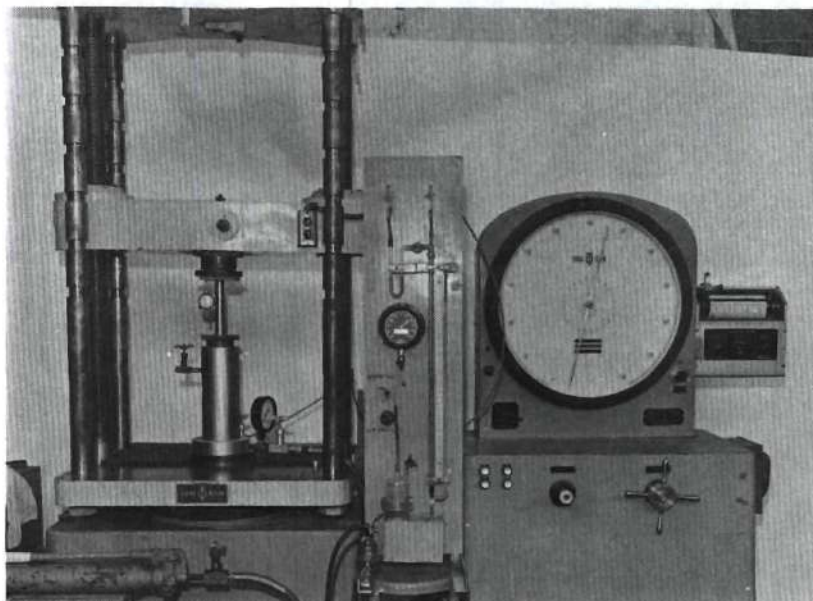


Figure 3. Triaxial Cell, Volume Change Device, and Testing Machine.

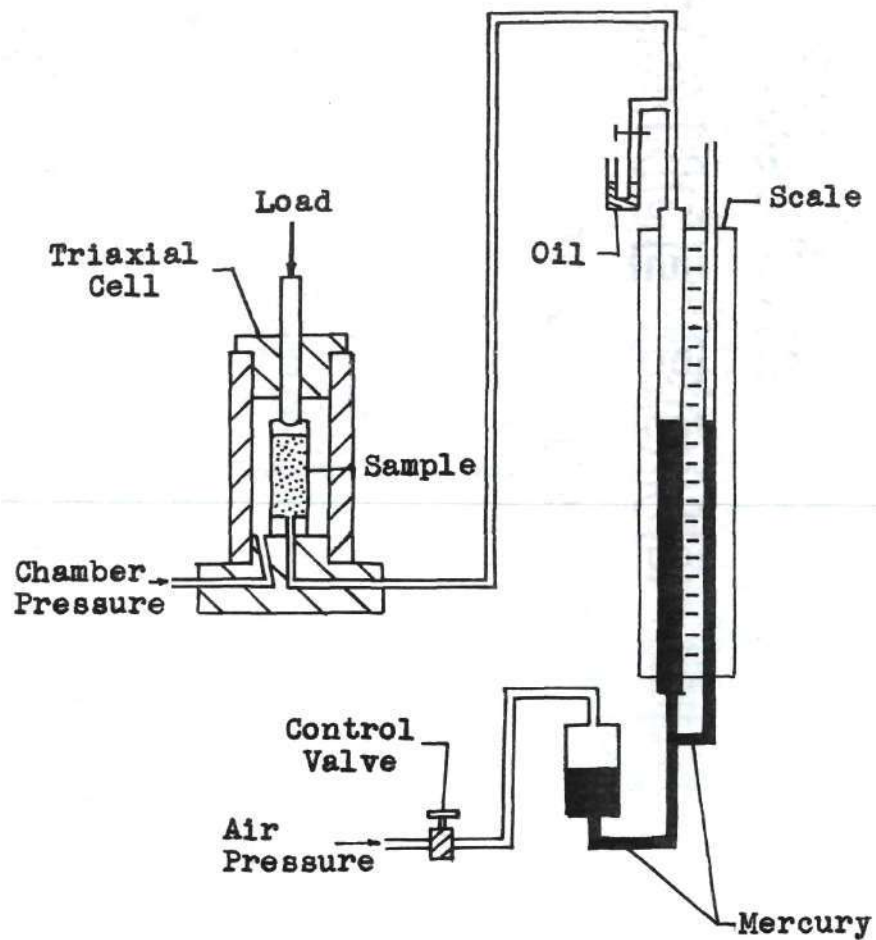


Figure 4. Schematic Diagram of Volume Change Device.

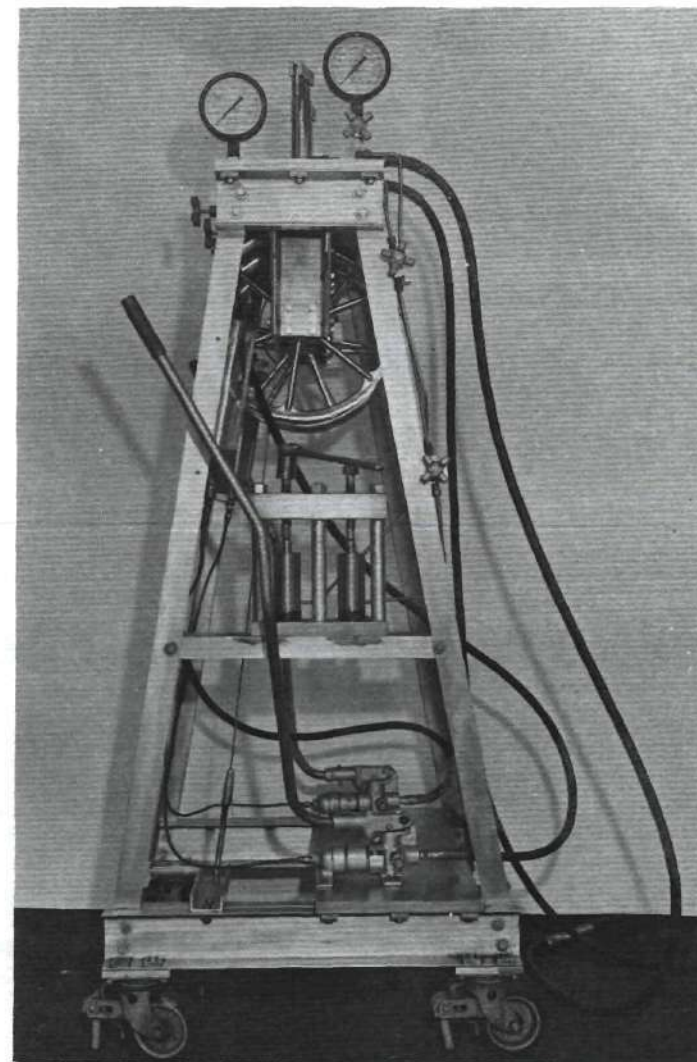


Figure 5. The Pressure Accumulator.

The air pressure acted upon the surface of the mercury exposed in the enlarged portion of the U-tube at the base of the burette.

As a check on the constant pressure air system device, a number of the tests were conducted with saturated samples whose volume change was read in a 100 cc burette connected to the pressure connection associated with the base of the sample.

The Pressure Accumulator

In the case of the constant octahedral normal stress tests, the confining pressure had to be necessarily closely controlled and regulated. The device used for this purpose was a pressure accumulator arranged so that the confining pressure could be adjusted by hand. It consisted of a cylinder and adjustable piston inserted into the system maintaining confining pressure so that movement by the piston caused an increase or decrease of volume in the system, thereby increasing or decreasing the pressure. The piston was adjusted by turning a threaded bolt which exerted pressure on the piston which was in turn being acted upon by the cell pressure. The cylinder was made of bearing bronze and the piston of high strength steel (See Figure 5). The original accumulator was designed by A. E. Schwartz (15) for high pressure tests on rock.

Loading Machines

Two loading machines were used in the tests, the one used depending on the load required to fail the sample. For loads up to 20,000 pounds, a mechanically driven machine was used at a constant strain rate of 0.02 inches per minute. Samples requiring higher loads were tested

in a hydraulically driven machine, manually controlled to attain a strain rate of 0.02 inches per minute. The hydraulic machine is shown in Figure 3.

Measurement of Sample Deformation

A micrometer dial indicator having divisions of 0.0001 inches was used to record sample deformations and, in the case of tests conducted on the hydraulic machine, was used also to control the rate of machine travel. The dial indicator was attached to a rod on a stand and placed against the crosshead of the loading machine as shown in Figure 3.

The Membrane

The membrane used at pressures above 20 kg. per sq. cm. was made of plasticized polyvinyl chloride with a two-inch inside diameter and a wall thickness of 0.055 inches. It is listed under military specifications as having a minimum tensile strength of 1,800 psi, a minimum elongation of 200 per cent, and a maximum elongation of 450 per cent.

A triaxial test at a confining pressure of 633 kg. per sq. cm. was conducted using bentonite clay at 300 per cent water content as a dummy sample inside the membrane. The bentonite has a strength of approximately five pounds in low pressure quick triaxial tests, but this test indicated it took 1,000 pounds to fail the sample. This 1,000 pounds then apparently was used to deform the membrane. The error would range from about 1 per cent at a confining pressure of 633 kg. per sq. cm. to about 4 per cent at a confining pressure of 211 kg. per sq. cm.

CHAPTER III

TESTING PROGRAM

The testing program can be divided into two categories:

(1) the tests conducted according to standard triaxial procedure, that is, a constant chamber pressure and application of a positive deviator stress to failure of the specimen,

(2) the tests conducted at a constant octahedral stress by a special procedure.

General Description of the Sand

The sand used in all tests was a subangular river sand obtained from the Chattahoochee River near Atlanta, Georgia. A microscopic examination of the sand revealed that mica particles were present, but that quartz grains were the dominate particles in the composition of the sand. The sand is characterized by a uniform gradation and is medium grained as can be seen from the grain size distribution curve.

The maximum density of the sand was found by compacting the dry sand vigorously by a hammer in five equal layers in a 1/30 cubic foot mold. The minimum density of the sand was ascertained by placing 1,000 grams of the sand in a graduated cylinder, tilting the cylinder to the horizontal position, and gently lowering it back into a vertical position. Reading the new volume and knowing the weight, the new density was calculated.

The other significant properties of the sand have been described

in detail in a published paper by Vesić (13) and are summarized in Table 1.

Table 1. Significant Properties of the Sand

Classification	
(Unified Soil Classification System)	Uniform Slightly Micaceous Sand
Coefficient of Uniformity	2.50
Mean Diameter	0.37 mm
Specific Gravity	2.66
Plasticity Index	Non Plastic
Maximum Density	104.5 lb. per cu. ft.
Void Ratio of Maximum Density	0.593
Minimum Density	79.8 lb. per ft. ³
Void Ratio of Minimum Density	1.09

Preparation of Samples

Dry Specimens--Dense

With the membrane firmly attached to the base by three O-rings, 1.75 inches in diameter, a forming jacket was placed around the membrane and a vacuum of about 5 psi was established to insure the proper cylindrical shape of the samples. The air dried sand was placed in five equal layers and tamped by a rubber-tipped rod. This procedure consistently gave a specimen with a void ratio of about 0.70. With the specimen height at approximately five inches, the top cap was placed on the sample and four O-rings were stretched around the membrane and top cap. This was apparently a sufficient seal to prevent leakage into the sample since no oil could be discerned on the inside of the membrane in any tests

prepared in this manner. After removal of the forming jacket, the sample dimensions were taken and void ratio calculated.

Saturated Specimens--Dense

The samples were prepared, as just described, in a dry condition but the cap used had a connection for a vacuum line on its side. A vacuum of about four psi was established on the sample in order to pull water through the sample from a water burette connected to the base. After all the visible trapped air had been removed from the system and the sample saturated, the forming jacket was removed and the specimen dimensions measured.

Dry Specimens--Loose

The membrane and forming jacket were arranged as before, but the sample was placed into the membrane by dropping the sand from zero height through a cylindrical tube with a sieve bottom slightly smaller than the membrane. At the proper height, the top cap, with silicone vacuum grease thoroughly coated on the sides, was carefully placed on the sample and two large rubber bands were stretched around the membrane, disturbing the sample as little as possible. The top cap was then pressed down again lightly on the sand surface which had dropped a small amount with the placement of the rubber bands. The forming jacket was then removed, sample dimensions measured, and void ratio calculated. This method of preparation consistently gave an average void ratio of 1.00. If the calculations revealed that the sample was not loose enough, the process was repeated.

The samples after failure were closely inspected for oil traces and only once was it found that the rubber bands had not prevented oil

from entering the sample. The consistency of the volume change results would also tend to substantiate this fact.

Saturated Specimens--Loose

As described in the previous methods, the membrane and forming jacket were prepared to receive the sample. A specific weight of sand was weighed out and dampened enough to give the sand some apparent cohesion. Carefully the sand was spooned into the membrane so as to take full advantage of the honeycombing effect developed by the apparent cohesion. Water was then forced into the bottom of the sample under the action of a small head of water in the burette connected to the base. Sand was added as the top of the sample subsided when the honeycombing collapsed. The end result, after complete saturation and the placement of the top cap, was a sample yielding an average void ratio of 1.00.

It should be mentioned here that in the case of the three tests run at confining pressures below 21 kg. per sq. cm. the procedure for preparation of the samples was the same as the appropriate one described above, but natural rubber membranes were used instead of the polyvinyl membrane. This change was made since first, it was only possible to do so below that pressure due to the weakness of the natural rubber and second, since the polyvinyl membrane might significantly affect the volume change results at lower pressures.

Assembly and Operation of the Testing Apparatus

Standard Triaxial Tests at High Pressures

After the specimen had been properly prepared and measured, the cylinder was tightened onto the base. Before adding the piston assem-

bly, hydraulic jack oil was filled up to the level of the valve in the top of the cylinder. The piston assembly was then appropriately tightened into the cylinder and the distance to the top of the sample was measured to be used later to determine how far the top of the sample deflected under confining pressure. At this juncture, the piston was pushed to the top of the sample and all excess air was bled out of the system through the valve at the top of the cylinder. Throughout all of these operations, the volume change device, which had been zeroed and connected from the beginning, was checked to note any disturbance to the sample. Before application of confining pressure, the volume change device was rezeroed and a dial indicator set up against the crosshead and zeroed. The confining pressure was then applied by a hand jack which forced oil through the entry port in the base.

The increments of confining pressure were limited by the amount of volume change that could be accommodated by the oil manometer of the volume change device. That is, volume decrease in the sample was reflected by an upward movement of the oil in the left leg of the U-tube which could not be allowed to proceed to the point where air escaped from the system. The oil level was brought to its original position by lowering the column of mercury through a decrease in the air pressure supporting the column. This action maintained atmospheric pressure in the pore space and the measuring system; thus, the overall volume of air in the system was constant and the mercury level in the burette gave a direct reading of volume change in the sample. The same increments used with the constant air pressure system were repeated when using the water burette to measure volume change to achieve uniformity in procedure.

Although the largest percentage of the volume change occurred immediately after an increment of pressure was added, the phenomenon of crushing of grains caused an extension in time required for complete consolidation. In fact, at higher pressures, it was found that an arbitrary point had to be chosen for volume change under a given increment. In order to be consistent, the reading at which less than 1/10 cubic centimeter of volume change was detected in 15 minutes was chosen as the final value. Several "standard" tests were run in which this same time interval was upped to one hour to check the error involved in this arbitrary cut-off point. As a comparison, it should be mentioned that in order to confine a sample to 9,000 psi and read volume change under the 15 minute limit, it took about 8 hours; whereas under the 1 hour limit, it took nearly 36 hours. The increased accuracy was not such that the additional time was justified.

When the application of confinement was completed, the new position of the top of the sample was determined by noting on the deformation indicator the point at which the sample began to take load. As the piston was brought down to the sample, the piston friction was zeroed out, thus eliminating a potential source of error. After properly zeroing the dial indicator, the volume change device, and the load machine, the shear test was performed. The load was read at a predetermined deformation as was the volume change, and the loading rate was continually checked to keep the rate as closely as possible to 0.02 inches per minute.

Any changes detected in confining pressure during the test were quickly corrected by either adding pressure by the hand jack or reducing

pressure by slightly cracking the relief valve on the jack.

Disassembling the cell at times required the use of a large open-end wrench cut especially for the hexagonal shape of the top of the piston assembly, but normally the cell could be dismantled by hand. After siphoning the oil from the cylinder, the specimen and the membrane were examined closely for any perceptible oil leaks. The remains of the samples were saved to be later used in a sieve analysis.

Constant Octahedral Stress Tests

Assembly of the cell and application of confining pressure was accomplished as in the procedure described for the standard triaxial tests, but the shear test was performed in a different manner. The octahedral normal stress is given by the equation:

$$\sigma_{\text{OCT}} = 1/3 (\sigma_1 + \sigma_2 + \sigma_3)$$

Thus, in the constant octahedral stress test, a predetermined increment of axial stress was added to the sample and, simultaneously, one-half of that stress increment was removed from the confining pressure. Since the axial stress depends on the cross-sectional area and this varies with deformation, a chart was prepared prior to the test of corrected cross-sectional area versus deformation.

During the test, the deformation required to reach the necessary axial stress increment was estimated and the corresponding cross-sectional area was multiplied times the stress value giving the required load for the sample. As the load was gradually increased, the confining pressure was gradually decreased by its specified increment using the

pressure accumulator. The actual deformation and the volume change were recorded during the test. Saturated samples were used in these tests due to the fact that the volume change device required no manipulation as the test was conducted and allowed full attention to be focused on the adjustment of the confining pressure. All tests were run at a strain rate of 0.015 inches per minute.

The Sieve Analysis

Material from the samples of each test was conserved and later combined with the material from like tests for a sieve analysis to increase the representativeness of the sieve analysis.

The Reduction of Data

The reduction of the data was accomplished through a computer program designed for the Burroughs 220 computer.

CHAPTER IV

DISCUSSION OF RESULTS

Reduction of Data

Compressing a sample under a high confining pressure involves a significant change in cross-sectional area and height of the sample, and thus must be considered when calculating stresses and strains. Of the two, only the change in height is directly measurable and the resulting cross-sectional area must be approximated. The approximation was made by dividing the volume found by subtracting the known change in volume under confinement from the original specimen volume by the new height, also corrected by subtracting the change in height under confinement from the original specimen height. This gave an average cross-sectional area which was less for the loose samples than the dense, causing the loose samples to have equal failure stresses with the dense even though they in general took slightly less load. The strains were also calculated with the corrected height.

Percentage volume changes under shear were calculated on the basis of the corrected volume immediately before shear and not the original volume. Volume decrease was taken as positive and volume increase taken as negative to remain consistent with conventions used for stress in soil media.

All other calculations were made on the basis of standard conventions used in soil mechanics.

Shear Strength Characteristics

Figure 6 is a plot of the stress circles for all shear tests conducted. The scatter of data was such that several special graphs designed to aid in selection of a strength envelope were drawn (See Figures 7, 8a, and 8b). The plot of $\frac{\sigma_1 - \sigma_3}{2}$ versus $\frac{\sigma_1 + \sigma_3}{2}$, Figure 7, resulted in a straight line passing through the origin. The tangent of the slope angle of this line is equivalent to the sine of the ϕ angle of the strength envelope, and the cohesion or shear strength intercept of the envelope is equal to the intercept of the ordinate, $\frac{\sigma_1 - \sigma_3}{2}$, divided by the cosine of the angle ϕ . The respective values obtained from this plot were, ϕ equal to 32.4 degrees and cohesion equal to zero.

This being the case, the question then is raised as to how the ϕ angle, as determined by a previous investigation (17), goes from 44 degrees for dense sand at pressures below 0.7 kg. per sq. cm. to 32.4 degrees at high pressures. This curvature may be seen in Figure 8a which emphasizes the low pressure range. The equation of a straight line on this plot is given by:

$$\frac{\sigma_1 - \sigma_3}{\sigma_3} = \frac{2 \sin \phi}{1 - \sin \phi} + \frac{2 \cos \phi}{1 - \sin \phi} \cdot c \cdot \frac{1}{\sigma_3}$$

from which cohesion and the ϕ angle may be found. Between the highest pressure and about 30 kg. per sq. cm., the envelope apparently remains straight, and below that, begins to assume a new direction. To further define this trend, Figure 8b was drawn to include data determined at low

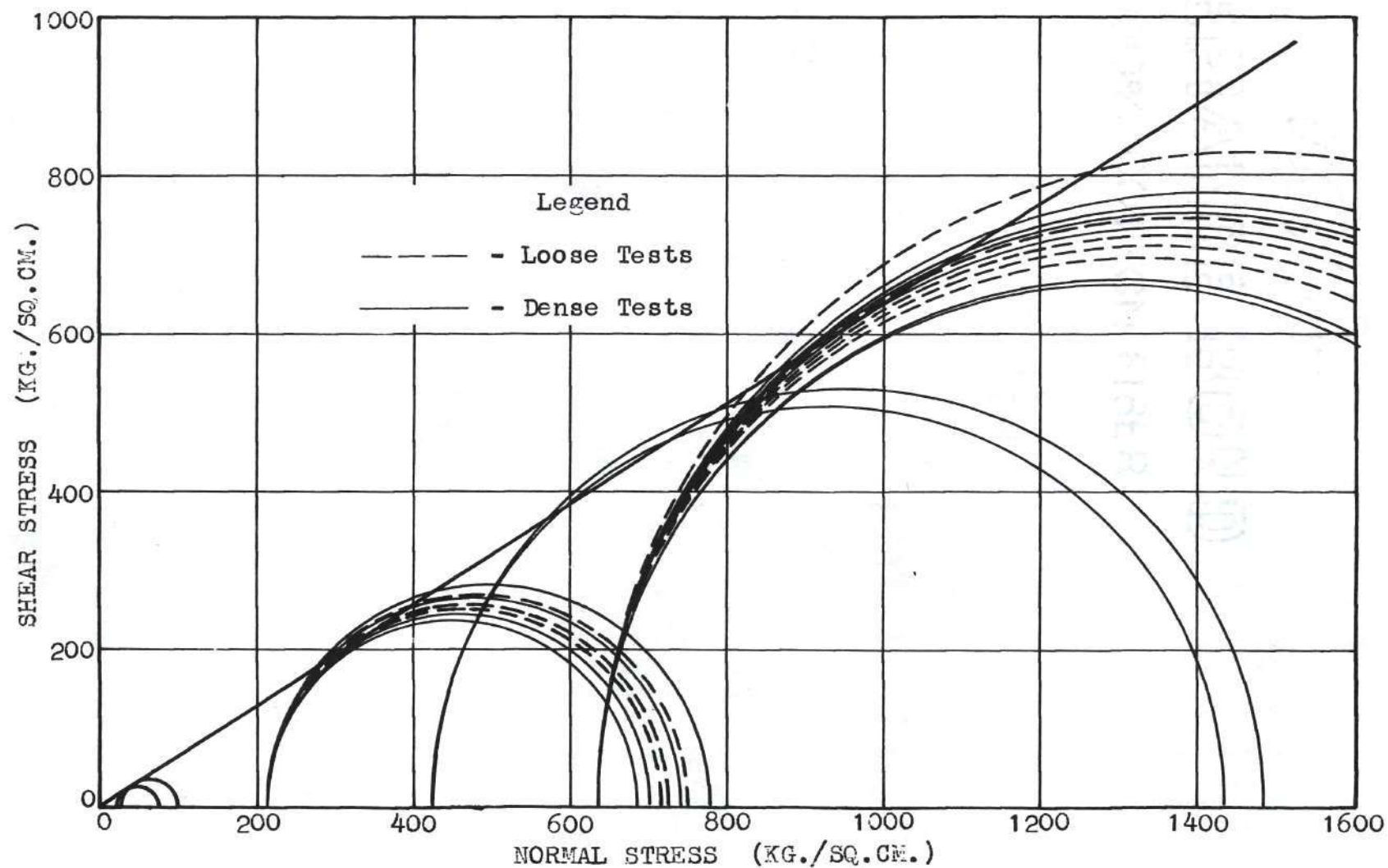


Fig. 6. Mohr Envelope and Stress Circles

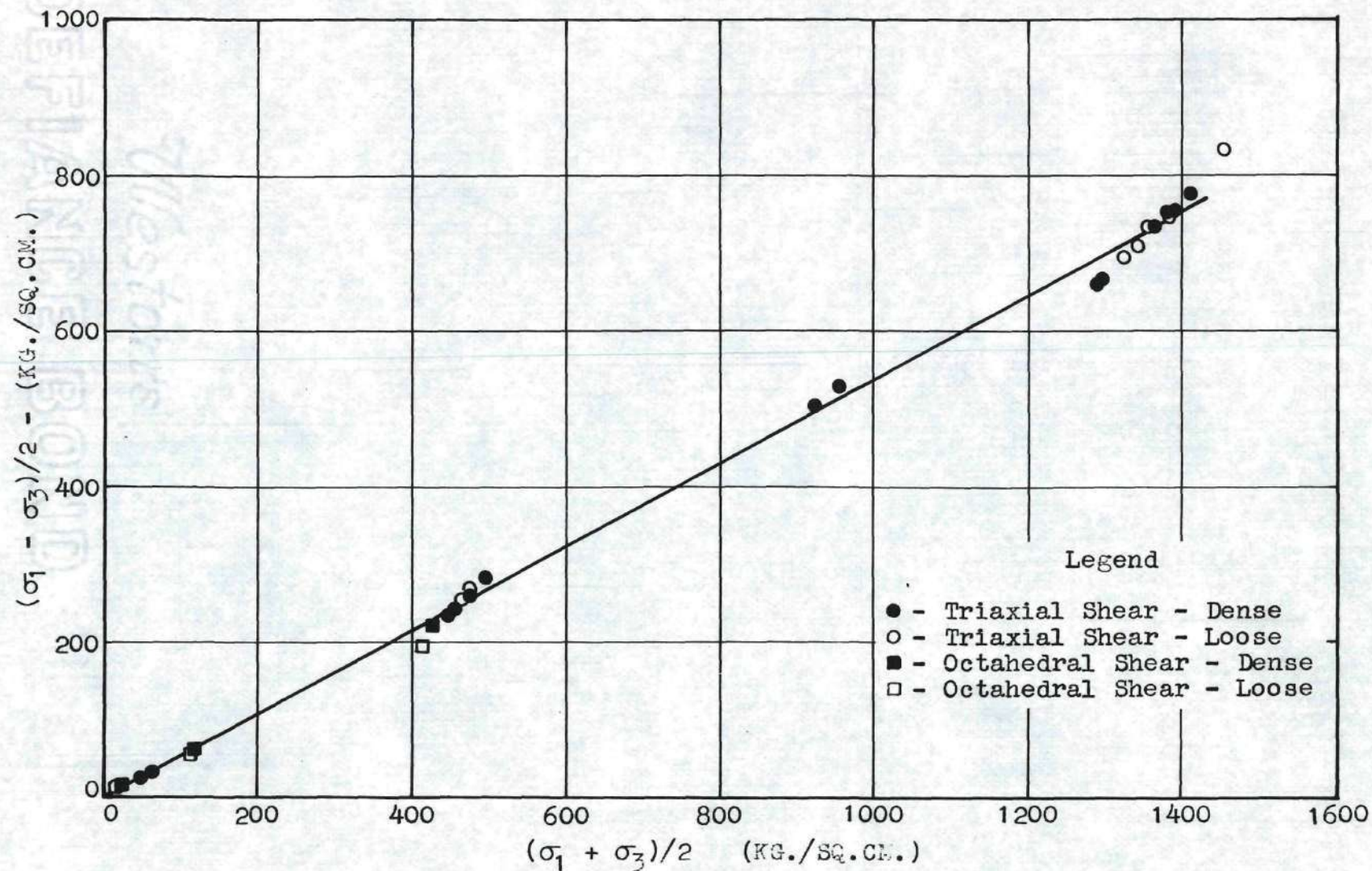


Fig. 7. $(\sigma_1 - \sigma_3)/2$ versus $(\sigma_1 + \sigma_3)/2$.

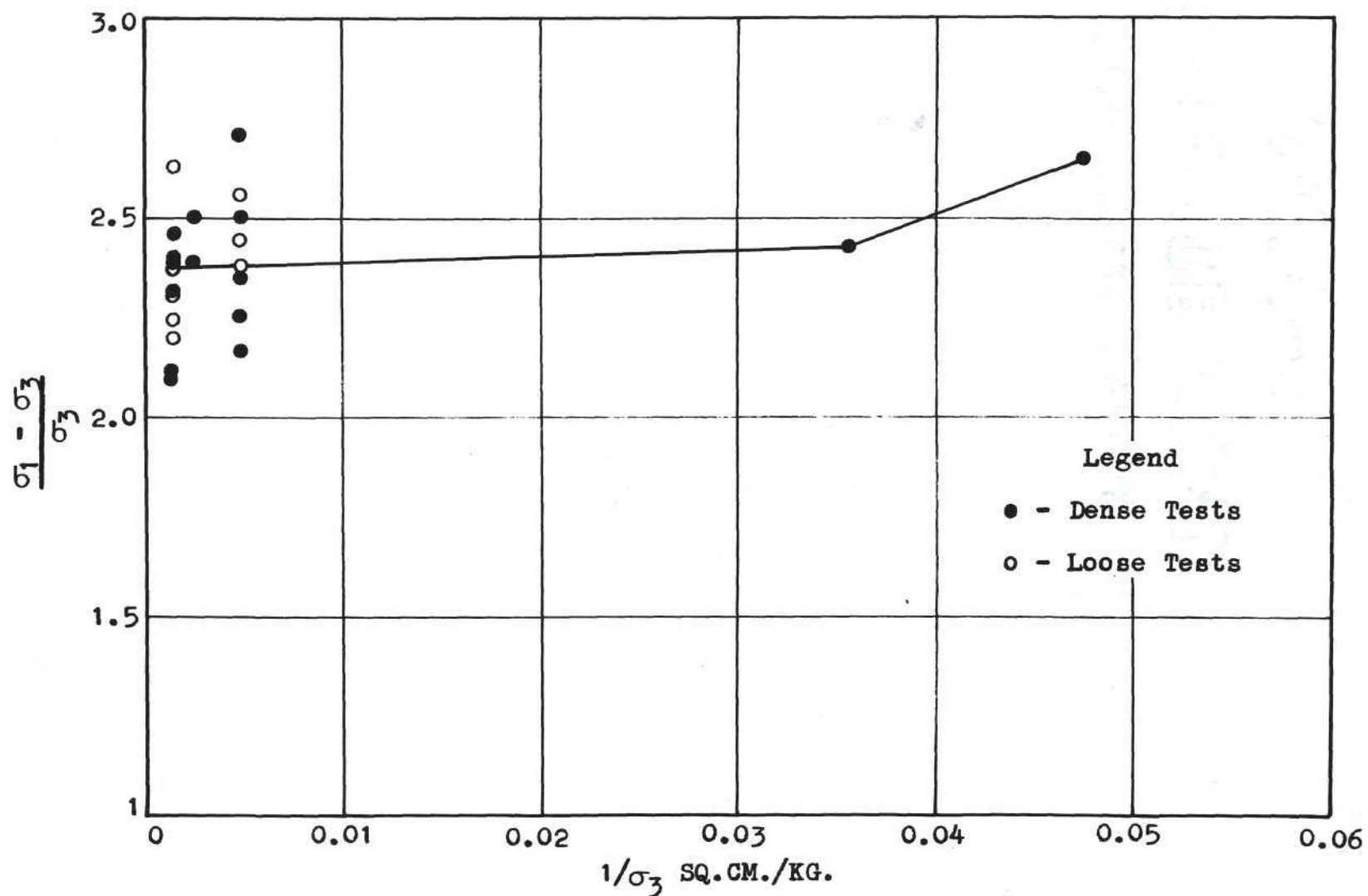


Fig. 8a. $(\sigma_1 - \sigma_3)/\sigma_3$ vs. $1/\sigma_3$.

pressures. The dashed curve is drawn between the available data, and its shape, of course, can only be inferred from the known points.

Thus, at least a good estimate may be made of the envelope curvature between 0 and 30 kg. per sq. cm. for the dense sand. The varying Φ angle values are summarized in Table 2.

Table 2. Characteristics of the Strength Envelope for Dense Sand

Range of Confining Pressures (kg. per sq. cm.)	Degrees
0. to 0.70	44.0
0.70 to 12.2	39.1
12.2 to 30.	27.9
30. to 633.	32.4

As the envelope is drawn in Figure 6, it is the same for both loose and dense sand, but this is not actually the case at low pressures. Using the data available from reference (13) and the shear circles from the octahedral tests, it may be predicted that the envelope for loose sands does not contain this wide departure from a straight line as in the case of dense sands (See Figures 8b, and 9). Two questions must then be asked: (1) What phenomenon causes the difference between the envelopes at low pressures which is not present at high pressures?

(2) Where does this difference cease to exist?

It is widely known that at low pressures a dense sand sample increases in volume under shear, a phenomenon termed "dilatancy." As explained by D. W. Taylor (16), positive work must be done to resist this volume increase, and thus additional load is required above that necessary to shear the soil resulting in an envelope curvature.

Since the curvature definitely varies as to intensity, it should follow that the dilatancy component of the shear strength also varies. To determine if this was the case, four constant octahedral normal stress tests were run on dense sand (See Figure 19). It should be explained that these tests should produce volume change only through shear and not by an increase in the compressive or normal stresses, thus isolating the effect to be investigated. From the constant normal octahedral stress tests plotted in Figure 19, the curve for dense sands shows that the dilatancy phenomenon is greatest at the low pressures and gradually decreases until about $\sigma_{OCT} = 30$ kg. per sq. cm., where it disappears. The parallel between this curve and the gradient of the curvature of the envelope for dense sand is revealing. It is greatest at the low pressures and then begins to decrease until, at about $\sigma_{OCT} = 50$ kg. per sq. cm., it disappears. These two values are closer than they appear when consideration is given to the difficulty of executing a constant octahedral test and the large range of pressures involved.

Also depicted in Figure 19 are the results from the loose tests with their initial void ratios listed beside them. The curve for these tests never goes to zero volumetric strain, and remains on the volume

decrease side of the graph in its entirety. This would indicate that the envelope for loose sands would have no significant curvature over the pressure range tested. As further proof, the reader is referred to Figure 8b which shows that the low pressure results on loose sand are correlated well with the high pressure data, all lying on one straight line. As could be predicted, the curves for dense and loose sand come together as the confining pressures get higher and only volume decrease is encountered for both sands.

Thus, as concluded by Vesić and Barksdale (11), it may be said that the dilatancy component of the shear strength of a dense sand significantly varies with the octahedral normal stress and, in fact, disappears at about 30 kg. per sq. cm., whereas the frictional component remains proportional to that stress over the entire range of pressures tested.

Volume Change Characteristics

Volume Change Under Confining Pressure

Curves of confining pressure versus volume change are shown in Figures 20 through 24. The ordinate of this curve could also appropriately be termed isotropic compression or octahedral normal stress since the meanings in this case are synonymous.

Certainly the bulk of the volume change takes place between $\sigma_3 = 0$ and 200 kg. per sq. cm. for both loose and dense samples after which it may be said the volume still decreases, but at a significantly lessening rate. The scatter between these curves may be attributed to small differences in initial void ratio, and in the case of the "stand-

ard" tests, Test 16 and Test 25, the time allowed for consolidation. For tests with comparable void ratios, the error for both loose and dense tests when compared to the "standard" tests was about 10 per cent from $\sigma_3 = 300$ kg. per sq. cm. to $\sigma_3 = 633$ kg. per sq. cm., and progressively less below $\sigma_3 = 300$ kg. per sq. cm. It is of significance to note that the saturated tests gave approximately the same results as the dry tests, adding to the reliability of the data.

The effect of time allowed for consolidation may be seen in the set of curves representing volume change versus time for a dense sand under different increments of confining pressure (Figure 25). There is a certain time lag before the pore pressure in the sample is dissipated and the volume change accomplished as evidenced by the reverse curvature in the early portion of the curves. It should be noted that the logarithmic scale exaggerates this effect. The volume change is due to both expulsion of the pore fluid under compression as well as continuing readjustment of the sample structure after crushing of the grains. Volume change under equal increments gets less as the pressure range gets higher because the sample gets progressively denser.

The peak of the curve requires more time to be reached as the pressures go above $\sigma_3 = 140$ kg. per sq. cm., probably due to the fact that the readjustment of grain structure continues for a longer period of time at higher pressures.

When the data from the two "standard" tests, Test 16 and Test 25, were plotted on log-log coordinates (Figure 26), there appeared to be two separate parts to each curve. First, there was a curved section which extended from $\sigma_3 = 0$ kg. per sq. cm. to about $\sigma_3 = 180$ kg. per sq.

cm., and second, there was an approximate straight line from $\sigma_3 = 180$ kg. per sq. cm. to $\sigma_3 = 633$ kg. per sq. cm. The slopes of the straight lines were nearly equal, indicating that beyond $\sigma_3 = 180$ kg. per sq. cm. the initial void ratio had no effect since both samples had reached the same state or void ratio. All of the volume change versus confining pressure curves show this distinct similarity beyond $\sigma_3 = 180$ kg. per sq. cm.

Volume Change in the Constant Octahedral Normal Stress Tests

Curves of volumetric strain versus octahedral normal stress for loose and dense tests are shown in Figure 19. Their significance with respect to shear strength has been discussed earlier in this chapter, but they have not been discussed as to volume change characteristics.

The curves for volumetric strain versus axial strain associated with each test are shown in Figure 27. A rather wide scatter of data occurred at $\sigma_{OCT} = 98.5$ kg. per sq. cm. and may be attributed to the unusually high variance between the initial void ratios.

In order to draw the curves in Figure 19 with a high degree of precision, more data would, of course, have to be added, but at least some inferences may be drawn from them. Significantly it may be noted that the two curves come together at approximately $\sigma_{OCT} = 200$ kg. per sq. cm. In a constant octahedral normal stress test, the sample is first confined to a given pressure and then the confining pressure reduced as the axial stress goes up. If a sample were confined to 200 kg. per sq. cm., the writer has found that both loose and dense samples have the same void ratio, thereby giving the same volume decrease under shear.

Volume Change in the Standard Triaxial Tests

In a standard triaxial test, volume change is being forced by two separate components, compressive stresses or octahedral normal stresses and shearing stresses or octahedral shearing stresses. With an increase in these components such as occurs in a conventional triaxial test, the volume change may be positive or negative depending on whether under the influence of the shearing stresses the volume increases and dominates the decrease due to increased normal stresses, or as higher pressures above 50 kg. per sq. cm., both cause a decrease. The amount of this decrease during the application of axial stress depends on the amount of previous confinement. Figure 28 shows the effect of confining pressure. From Figures 19 and 26, the shape of this curve may be explained since Figure 26 represents volume change under octahedral normal stresses, and Figure 19 represents volume change under octahedral shearing stresses, the two components isolated.

As could be expected, the volume change for both loose and dense samples at $\sigma_3 = 210.9$ kg. per sq. cm. was roughly the same, perhaps a bit higher for the loose samples. This could have been foretold since it was stated previously that the volume change under the separate influence of octahedral normal and octahedral shearing stresses became the same for loose and dense samples after confinement under 200 kg. per sq. cm.

As can be seen in Figure 28, in conventional triaxial tests above confinement of 210 kg. per sq. cm. the total volume change decreases rapidly between $\sigma_3 = 210$ and 400 kg. per sq. cm., then more slowly to $\sigma_3 = 630$ kg. per sq. cm. Consideration of the variation of the separate

entities of triaxial volume change in these pressure ranges provides an explanation of this behavior. Figure 19 shows that volume change under shear leveled off considerably above $\sigma_3 = 150$ kg. per sq. cm., thus above this pressure the curvature in Figure 28 depends largely on changes due to octahedral normal stresses. It has been noted previously that much of the volume change under increasing octahedral normal stresses took place before $\sigma_3 = 200$ kg. per sq. cm., after which the relationship between octahedral normal stress and confining pressure steepened sharply, so much so that progressively higher increases in octahedral normal stresses produced lessening increments of volume change.

Let us again refer to Figure 28 with the foregoing variations of volume change with confining pressure in mind. The curve in this figure is subject to the same curvature predicted by the discussion on the relationship between increasing octahedral normal stresses and volume change up to about $\sigma_3 = 400$ kg. per sq. cm., after which the changes in octahedral normal stresses become minor compared to the relatively steady volume changes under shear. Thus, beyond this confining pressure, the relationship in Figure 28 becomes more subject to the volume change variation under shear and levels off.

Actual values of volume change for the triaxial tests have been computed by superimposing the two components, using the strength data from the triaxial tests. They are summarized in Table 3. The triaxial tests above $\sigma_3 = 210.9$ kg. per sq. cm. could not be used in the calculations since their octahedral normal stress at failure was beyond the range of the curves available. The plots of the "standard" tests, Test 16 and Test 25 (Figure 26), on log-log co-ordinates were corrected by

constant values and fitted to straight lines with the following equations respectively:

$$(1) \quad \sigma_3 = 0.58 \frac{\Delta V}{V}^{2.1} + 4 \quad \dots \text{Test 16}$$

$$(2) \quad \sigma_3 = 0.0106 \frac{\Delta V}{V}^3 + 6 \quad \dots \text{Test 25}$$

where σ_3 = confining pressure in kg. per sq. cm. and $\frac{\Delta V}{V}$ = volumetric strain in percent.

Equation (1) was used for dense tests and Equation (2) for loose tests in the calculations of volumetric strain due to variations in octahedral normal stress. It should be noted that neither equation is necessarily applicable to very low pressures or to pressures above 633 kg. per sq. cm.

From the results presented, apparently the two separate components can be superimposed to give the volume change in a triaxial test. Certainly, a more thorough investigation would be in order to establish the validity of this finding.

The Effect of Initial Void Ratio

The initial void ratio, that is, the void ratio before any disturbance of the sample, has been shown to have no effect on shear strength characteristics above $\sigma_3 = 50$ kg. per sq. cm. As to volume change characteristics, it was stated that above $\sigma_3 = 200$ kg. per sq. cm. the dense and loose samples had the same void ratio and thus had no effect above that pressure. Table 4 is a compilation of the void ratios

Table 3. Superposition of Volume Change Components

Test No.	Initial σ_{OCT} kg. per sq. cm.	Final σ_{OCT} kg. per sq. cm.	Change in σ_{OCT} kg. per sq. cm.	$\frac{\Delta V}{V}$ Due to Normal Stresses Per Cent	$\frac{\Delta V}{V}$ Due to Shearing Stresses Per Cent	Volume Change Superposition Per Cent	Actual $\frac{\Delta V}{V}$ Per Cent
3	210.9	374.7	163.8	5.2	8.0	13.2	13.0
4	210.9	368.9	158.0	5.1	8.0	13.1	12.3
5	210.9	386.7	175.8	5.5	8.0	13.5	12.8
6	210.9	401.1	190.2	5.7	8.0	13.7	12.8
8	210.9	378.4	167.5	5.4	8.0	13.4	13.0
9	210.9	382.7	171.8	5.5	8.0	13.5	13.2
10	210.9	390.8	179.9	5.6	8.1	13.7	13.6
26	28.1	51.2	23.1	2.7	2.5	5.2	9.5
27	21.1	39.0	17.9	1.6	1.0	2.6	5.5

Table 4. Summary of Initial and Final Void Ratios

Test No.	e_i	Confining Pressure kg. per sq. cm.	$\frac{\Delta V}{V}$ Per Cent	e_f
1	0.78	210.9	14.5	0.52
2	0.80	210.9	18.0	0.48
3	0.70	210.9	13.3	0.47
4	0.72	210.9	17.0	0.43
5	0.67	210.9	18.4	0.36
6	0.68	210.9	14.3	0.44
7	1.04	210.9	27.7	0.47
8	0.99	210.9	25.6	0.48
9	1.01	210.9	27.1	0.47
10	1.00	210.9	27.4	0.45
11	0.77	632.8	23.4	0.35
12	0.73	632.8	22.7	0.33
13	0.71	632.8	22.8	0.33
14	0.72	632.8	24.4	0.30
15	0.71	632.8	23.3	0.32
16	0.67	632.8	26.4	0.23
17	0.68	632.8	23.3	0.28
18	0.72	632.8	23.6	0.31
19	0.99	632.8	35.1	0.29
20	0.99	632.8	33.0	0.34
21	0.91	632.8	31.1	0.31
22	1.00	632.8	31.9	0.35
23	0.99	632.8	32.2	0.35
24	0.94	632.8	35.5	0.26
25	0.99	632.8	36.2	0.27
26	0.70	28.1	4.7	0.62
27	0.69	21.1	3.6	0.63
28	0.72	21.1	3.5	0.66
29	0.61	98.5	11.2	0.43
30	0.69	351.0	22.1	0.32
31	0.69	1.0	0	0.69
32	1.02	21.1	6.4	0.88
33	1.06	98.5	24.6	0.55
34	0.93	351.0	28.8	0.38
35	0.94	1.0	5.5	0.83
36	0.66	421.8	21.5	0.30
37	0.64	421.8	22.1	0.28

before confinement and after. The average void ratios of loose and dense samples at $\sigma_3 = 210.8$ kg. per sq. cm. before confinement were 0.72 and 1.01, respectively, while after confinement they were 0.45 and 0.47. Tests above $\sigma_3 = 210.8$ kg. per sq. cm. gave similar agreement between before and after values, but at pressures as high as $\sigma_3 = 98.5$ kg. per sq. cm. there was still significant difference between the final void ratios after confinement.

Crushing of the Grains

Grain size distribution curves in Figure 29 illustrate quite pointedly the magnitude of the crushing of grains in triaxial shear. The phenomenon begins at relatively low confining pressures, crushing having been observed at $\sigma_3 = 21.1$ kg. per sq. cm. As the confining pressures increased, the crushing of grains became more prevalent. Apparently, as confining pressure goes above $\sigma_3 = 210.8$ kg. per sq. cm., the crushing effect does not go up as rapidly as it did up to $\sigma_3 = 210.8$ kg. per sq. cm. A more tangible insight to the crushing of the grains may be had by examining the optical micrographs shown in Figures 30 and 31. Figure 30 is a micrograph of two particles of the original sand, which have approximately the mean diameter of 0.37 mm, magnified 70 times. Figure 31 is a micrograph of a representative sample of the sand after confining and shearing at $\sigma_3 = 633$ kg. per sq. cm. magnified as in Figure 30, 70 times.

Loose and dense samples gave almost exactly the same distribution curves after shearing, indicating that initial void ratio has no effect on crushing of grains at high pressures. Comparative results between

the dry and saturated samples show some deviation, but this deviation is not outside the limits of data scatter in tests of these type and is not thought to be of any significance.

Figure 32 illustrates the effect of shearing the sand as compared to only application of chamber pressure. The sheared sand at $\sigma_3 = 210.8$ kg. per sq. cm. is in a much finer state than is the sand confined only to $\sigma_3 = 632.8$ kg. per sq. cm. This finding would substantiate the suggestion made by De Beer (8) that shearing forces account for crushing of grains as well as pure compressive forces.

Failure Strains and Failure Modes

Failure strain is defined as the strain corresponding to the peak-point stress. All of the tests tended to fail at strains above 20 per cent, with the tests at $\sigma_3 = 210.9$ kg. per sq. cm. generally failing at a higher strain than tests at pressures in higher ranges.

The samples failed largely by bulging although a shearing plane could be seen on a few of the samples. Two examples of the bulging failure are shown in Figures 33 and 34.

The Modulus of Elasticity

The variation of the initial tangent modulus of deformation with confining pressure is shown in Figure 35. There is a wide scattering of the data which makes it difficult to determine any exact relationship, but apparently it is not linear. Fitting a straight line to the points on log-log co-ordinates produces the following relationship:

$$E = 180 \cdot \sigma_3^{0.61}$$

where E = tangent modulus of elasticity in kg. per sq. cm. and σ_3 = confining pressure in kg. per sq. cm.

A second modulus of elasticity, which may be termed modulus of elasticity in isotropic compression, may be calculated using volume change data with an assumed Poisson's ratio in the expression

$$E_i = \frac{3\sigma_3 (1-2\nu)}{\Delta V/V}$$

where

E_i = modulus of elasticity in isotropic compression in kg. per sq. cm.

σ_3 = confining pressure.

ν = Poisson's ratio.

$\Delta V/V$ = volumetric strain (17).

The only Poisson's ratio which gave values of the modulus in isotropic compression which are comparable to the initial tangent modulus values was zero, which is not an accepted value for sand. Thus, it must be concluded that no particular relationship exists between the two moduli. Values of the two moduli may be seen in Table 5.

Properties of the Sand at Confining Pressures
Greater than 633 kg. per sq. cm.

It is conceivable that the sand might be confined to the point at which all the voids would be eliminated. From the volume change versus

Table 5. Comparison of Initial Tangent Modulus of Elasticity
to Modulus of Elasticity in Isotropic Compression

Assumed Poisson's Ratio	= 0	= 0.25	= 0.33	= 0.40	Initial Tangent Modulus
Test No.	E_i kg. per sq. cm.	E_i kg. per sq. cm.	E_i kg. per sq. cm.	E_i kg. per sq. cm.	kg. per sq. cm.
3	4,750	2,370	1,615	950	3,200
4	3,840	1,870	1,270	746	3,580
5	3,435	1,720	1,168	686	3,320
6	4,465	2,230	1,520	893	4,490
8	2,470	1,235	840	494	3,130
9	2,335	1,165	794	466	3,350
10	2,305	1,150	784	461	4,320
13	8,340	4,160	2,840	1,665	8,410
14	7,770	3,890	2,640	1,555	9,730
15	8,160	4,080	2,770	1,630	9,900
16	7,200	3,600	2,450	1,440	15,750
17	8,160	4,080	2,770	1,630	11,410
18	8,050	4,030	2,735	1,610	14,050
21	6,090	3,045	2,070	1,220	9,100
22	5,950	2,975	2,020	1,190	9,140
23	5,900	2,950	2,005	1,180	8,600
24	5,350	2,675	1,820	1,070	9,960
25	5,250	2,620	1,780	1,050	10,600
26	1,795	900	610	359	2,380
27	1,760	880	600	352	1,270
36	5,750	2,880	1,955	1,150	7,500
37	5,580	2,790	1,900	1,118	7,350

confining pressure plots, it can be seen that the upward curvature is still slightly increasing even above $\sigma_3 = \text{kg. per sq. cm.}$, thus, in order to reach zero voids, which for Test 16 and Test 25 would represent 40.1 per cent and 50.0 per cent volumetric strain, the curve would practically approach this maximum volumetric strain as if it were an asymptote. From the equations determined from Figure 26 representing Tests 16 and 25, values of pressure for the given final volumetric strains could be calculated, but they do not take into account the final upward curvature of the relationship which probably increases still more above the limiting pressures used in this investigation.

When sufficient pressure had been reached to eliminate the voids, the sand would actually be quartz. Triaxial tests up to $\sigma_3 = 24,600 \text{ kg. per sq. cm.}$ run on quartz have established the ϕ angle to be 13.25° and the cohesion to be $9,250 \text{ kg. per sq. cm.}$ (18). Thus, from the ϕ for sand of 32.4° at $633 \text{ kg. per sq. cm.}$ the envelope could be expected to curve downward to reach 13.25° . The extrapolated envelope is shown in Figure 36.

CHAPTER V

CONCLUSIONS

The conclusions drawn from this investigation must be in some cases generalized since not all of the effects were clearly distinguished, based on the tests available. All of the conclusions are of necessity based on the Chattahoochee River sand tested.

1. The strength envelope for both loose and dense sand in the pressure range from 50 kg. per sq. cm. to 633 kg. per sq. cm. may be approximated by a straight line and has a slope angle of 32.4 degrees.

2. The strength envelope for dense sand has significant curvature between 0 and approximately 50 kg. per sq. cm. due primarily to dilatation.

3. Initial void ratio ceases to affect shear strength characteristics above 50 kg. per sq. cm., and volume change characteristics above 200 kg. per sq. cm.

4. Crushing of grains becomes an important phenomenon at chamber pressures as low as 21.1 kg. per sq. cm. and increases, but not linearly, with confining pressure.

5. Crushing of grains is increased by application of shearing forces to an isotropically confined sample.

6. There are indications that the volume change under shear alone in a triaxial test may be found by subtracting from the volume change found in a triaxial test the appropriate volume change in an isotropic

compression test corresponding to the increase in octahedral normal stress in the triaxial test.

7. Volume change throughout shear for loose sands is a decrease from chamber pressures of 0 to 633 kg. per sq. cm.; whereas, for a dense sand volume increases from chamber pressures of 0 to about 30 kg. per sq. cm., and decreases past 30 kg. per sq. cm.

CHAPTER VI

RECOMMENDATIONS FOR FURTHER STUDY

1. An extensive series of constant octahedral shear tests should be conducted so that the relationship between octahedral normal stress and volume change under shear may be more specifically defined.
2. Variations in shear strength and volume change characteristics of clays at high pressures present an interesting topic for further study.
3. Even higher pressures than 633 kg. per sq. cm. should be employed in the testing of sands.

APPENDIX

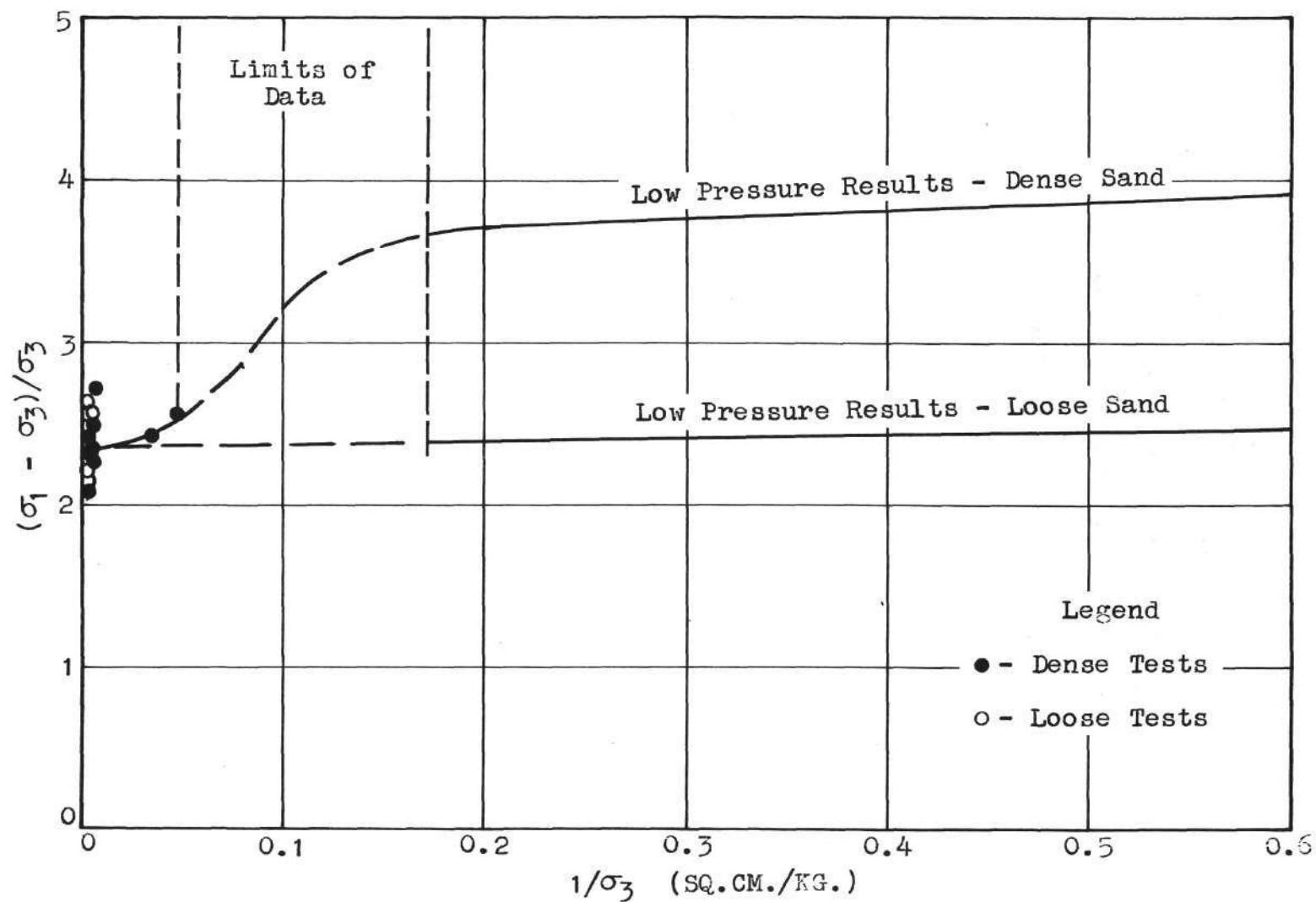


Fig. 8b. $(\sigma_1 - \sigma_3)/\sigma_3$ vs. $1/\sigma_3$.

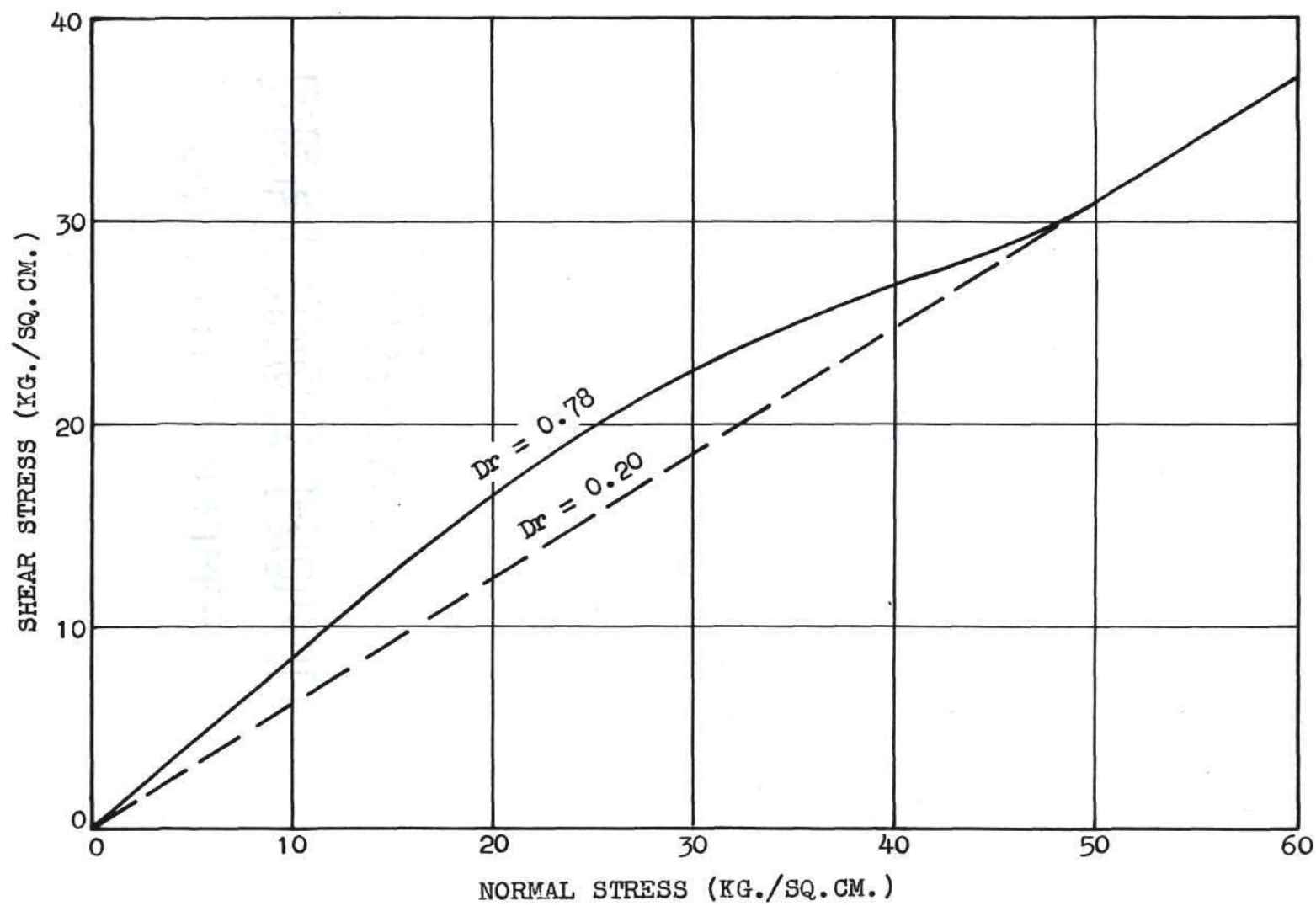


Fig. 9. Mohr Envelopes for Loose and Dense Sand at Low Pressures.

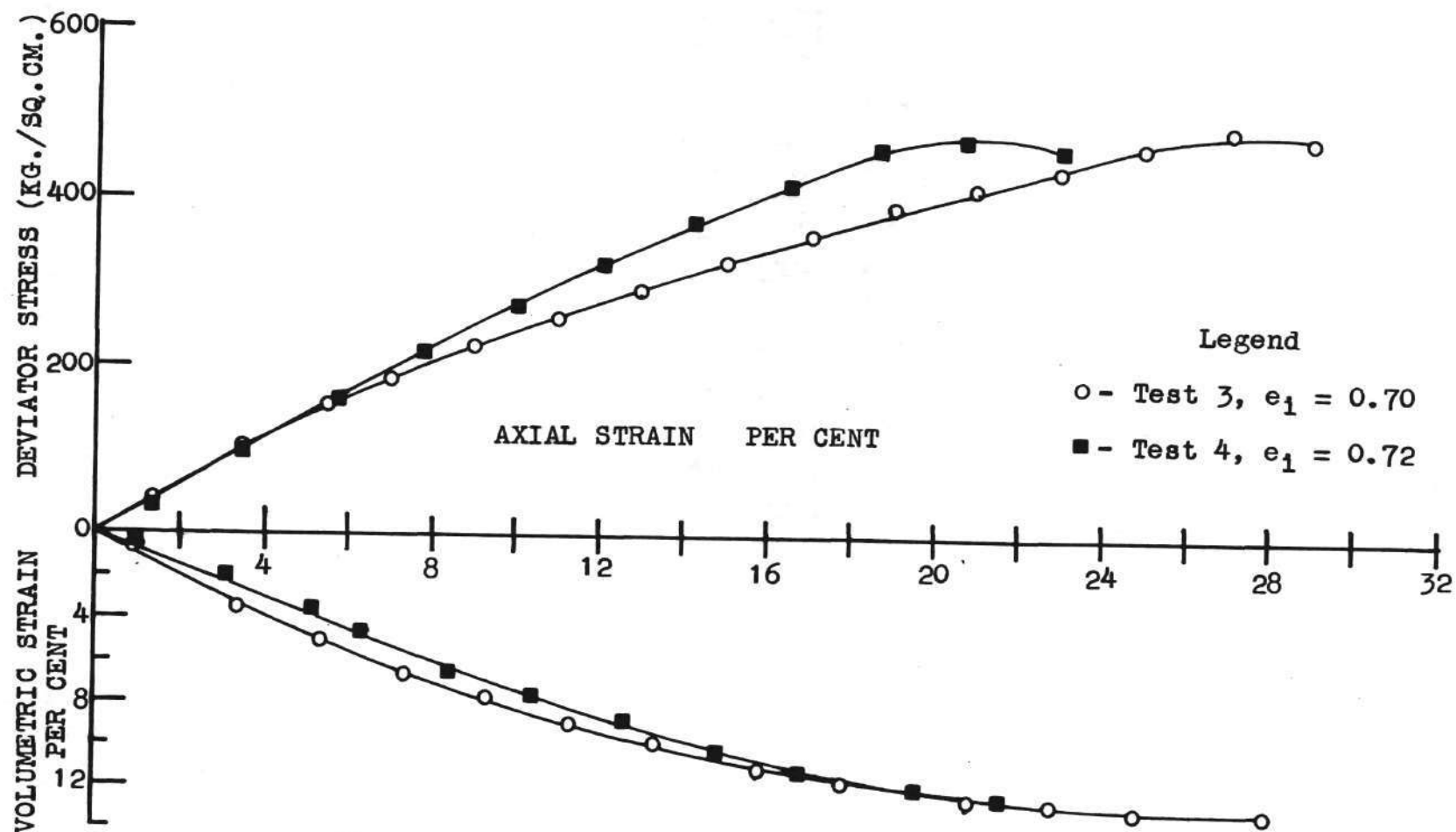


Fig. 10. Stress-Strain Curves at $\sigma_3 = 210.9$ kg./sq.cm.

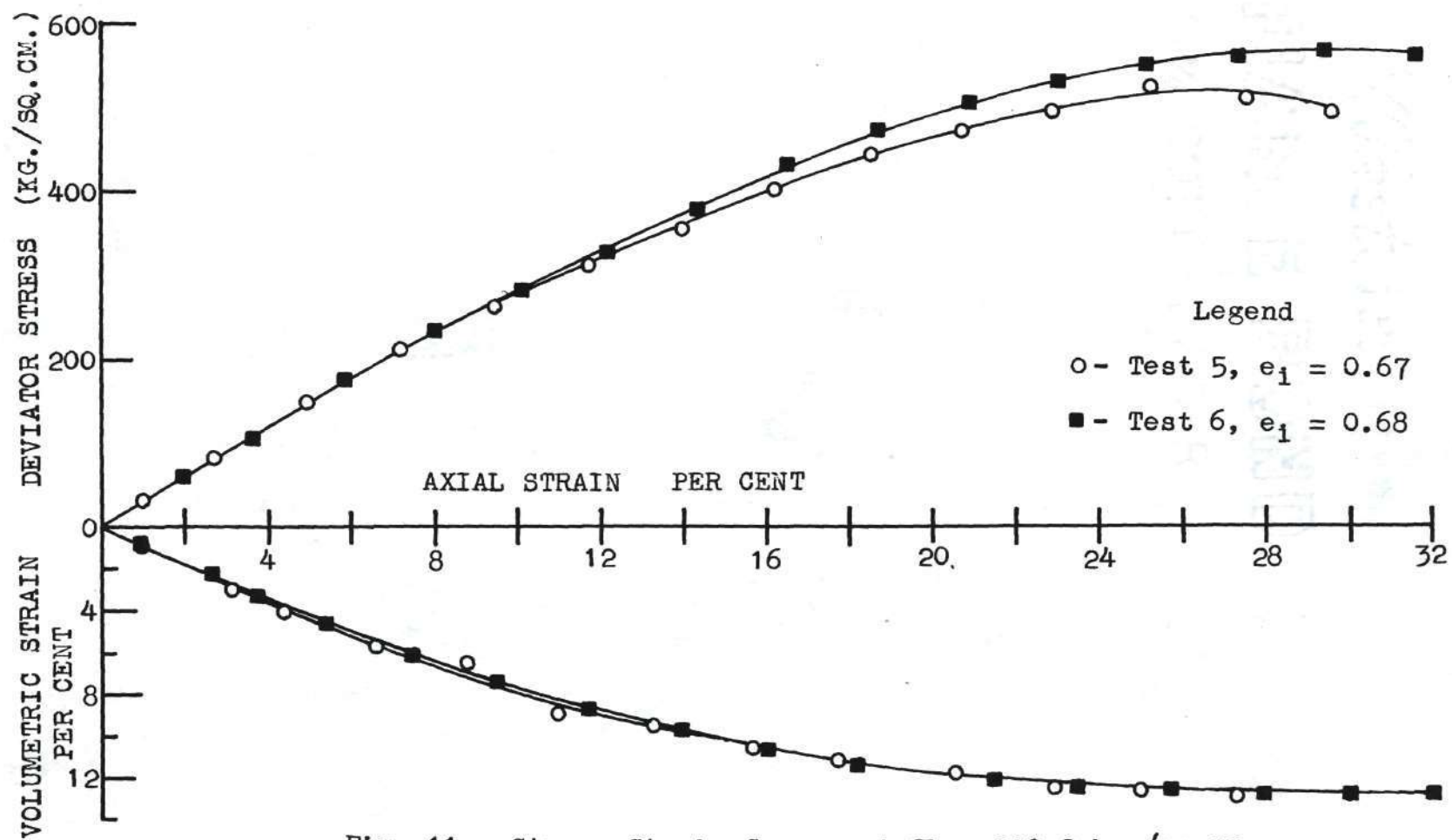


Fig. 11. Stress-Strain Curves at $\sigma_3 = 210.9$ kg./sq.cm.

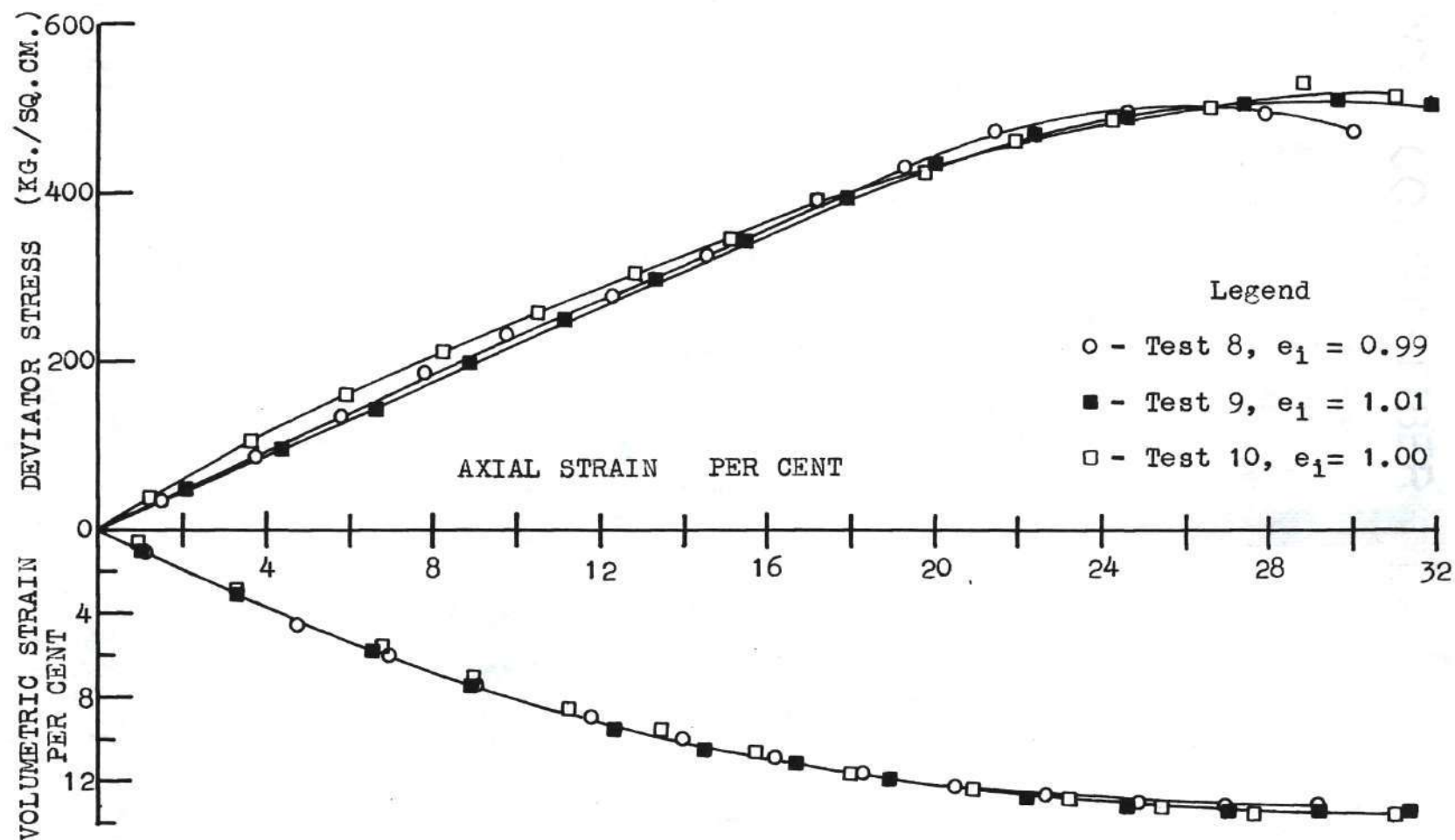


Fig. 12. Stress-Strain Curves at $\sigma_3 = 210.9$ kg./sq.cm.

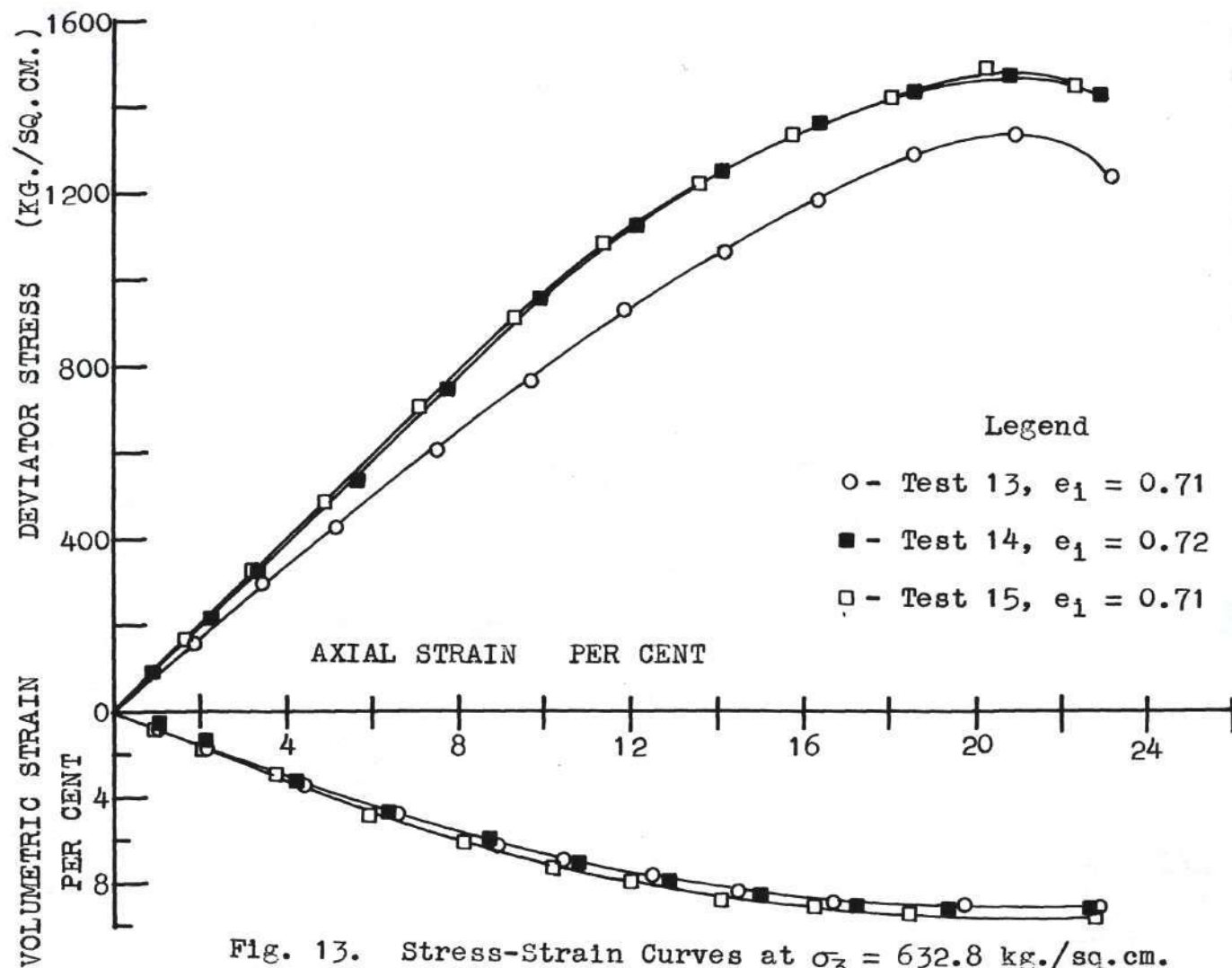


Fig. 13. Stress-Strain Curves at $\sigma_3 = 632.8$ kg./sq.cm.

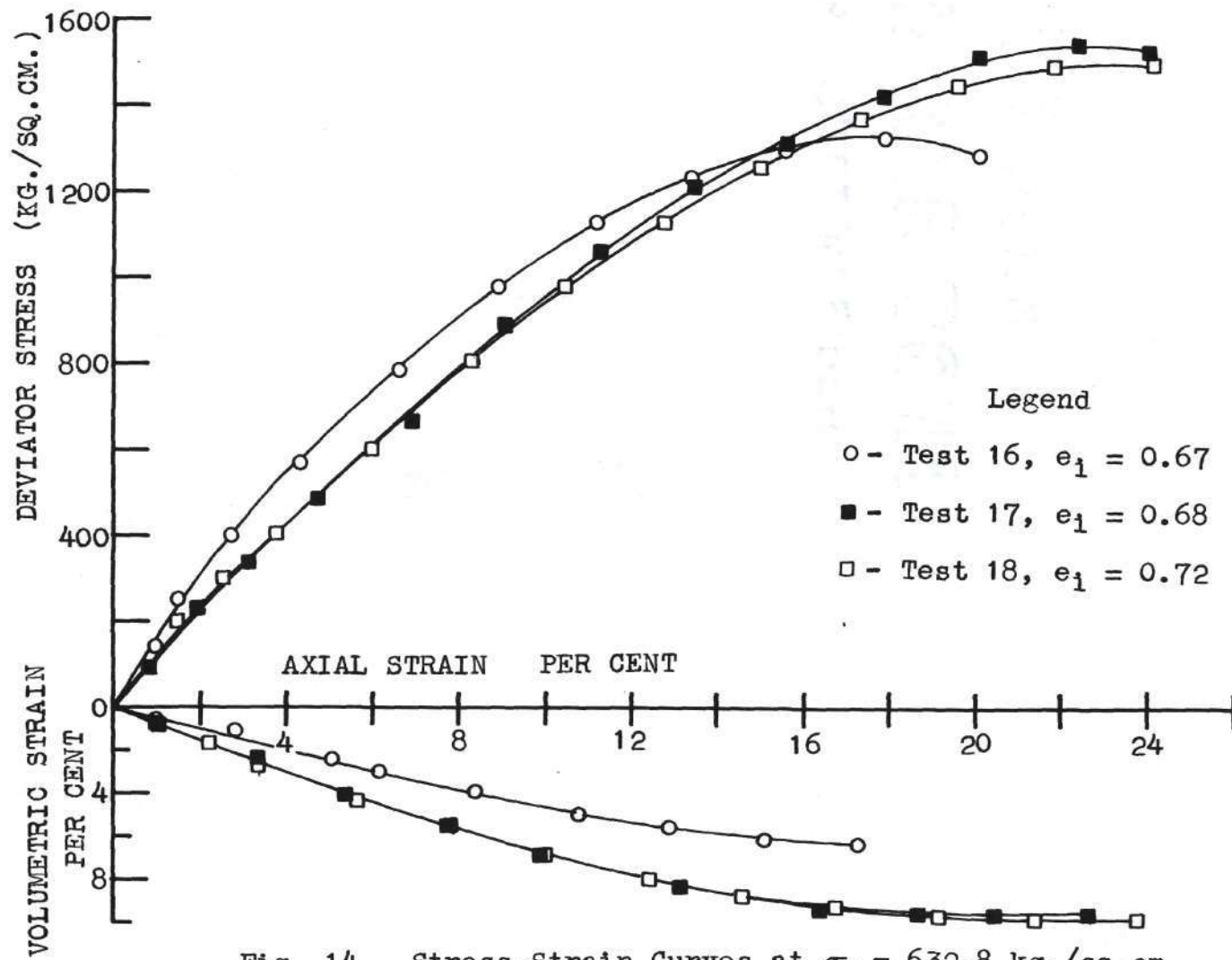


Fig. 14. Stress-Strain Curves at $\sigma_3 = 632.8$ kg./sq.cm.

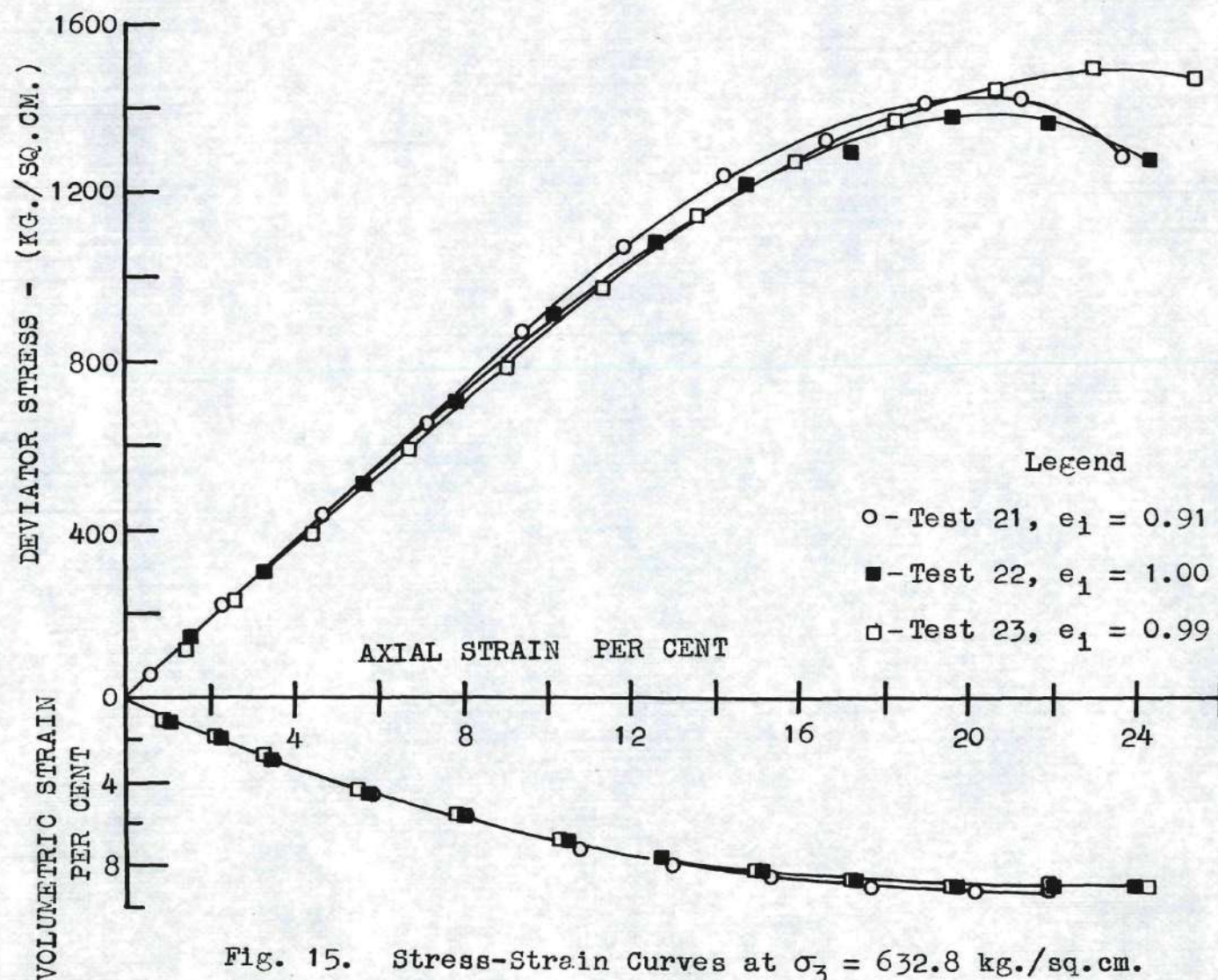


Fig. 15. Stress-Strain Curves at $\sigma_3 = 632.8$ kg./sq.cm.

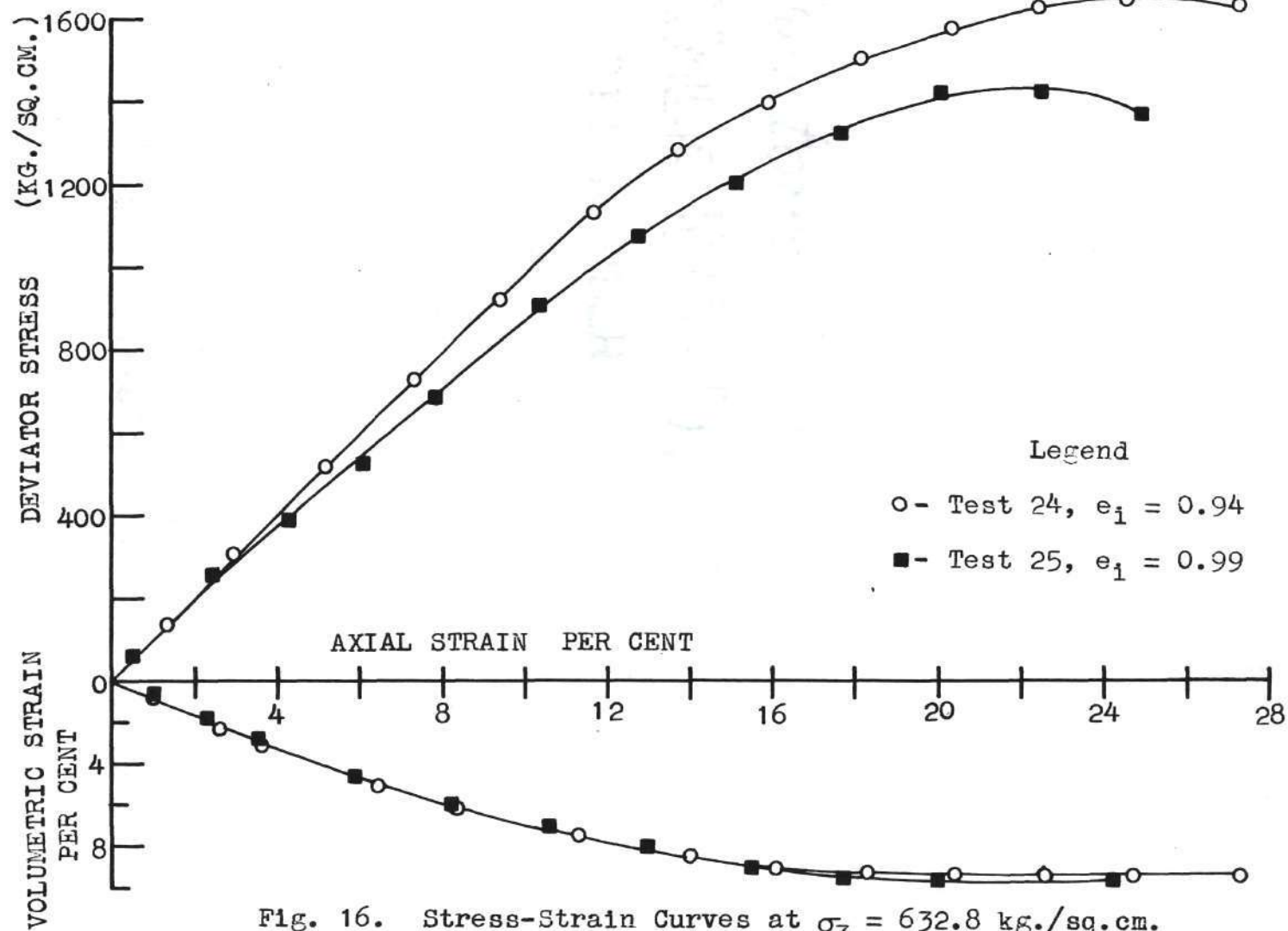


Fig. 16. Stress-Strain Curves at $\sigma_3 = 632.8$ kg./sq.cm.

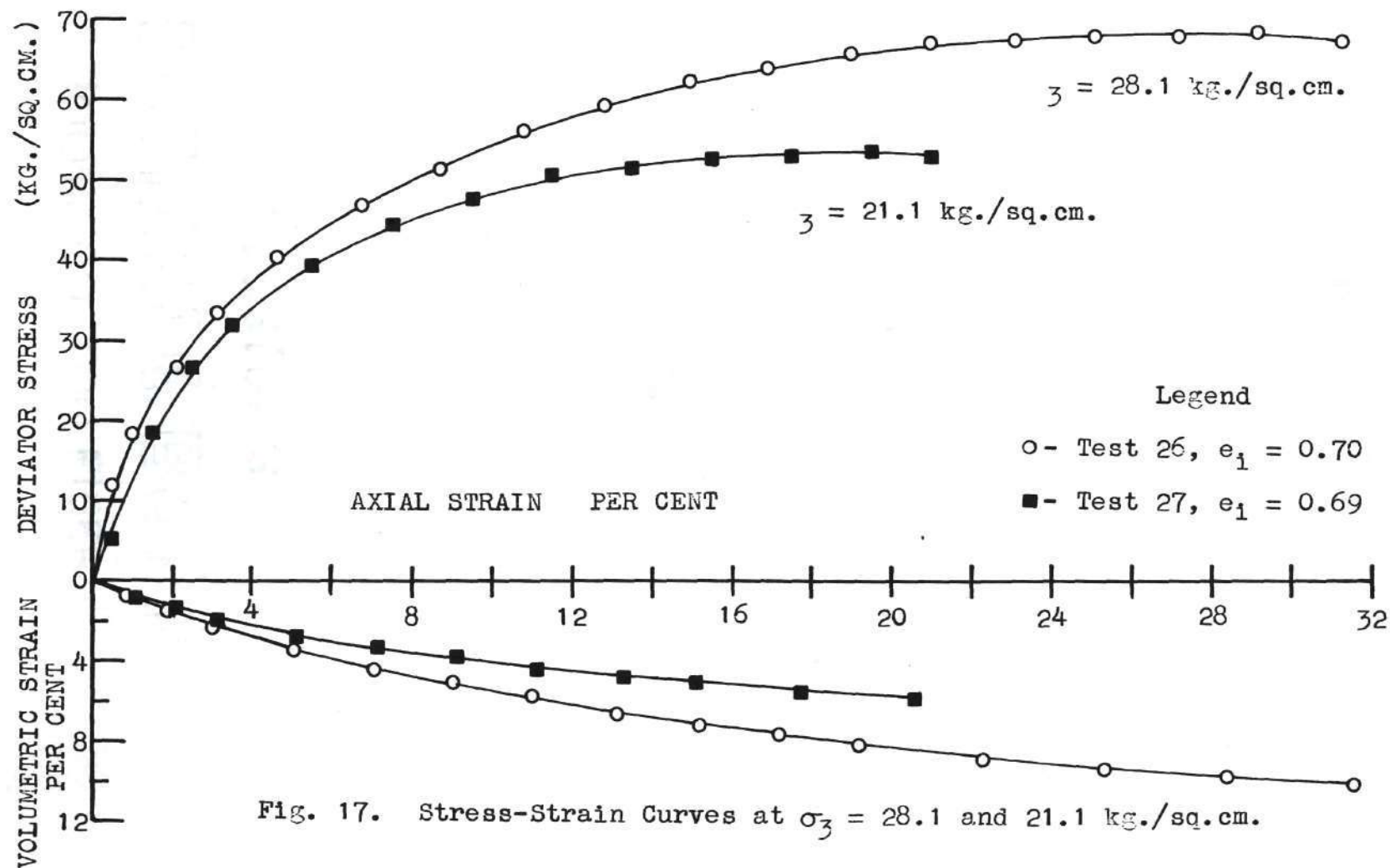


Fig. 17. Stress-Strain Curves at $\sigma_3 = 28.1$ and 21.1 kg./sq.cm.

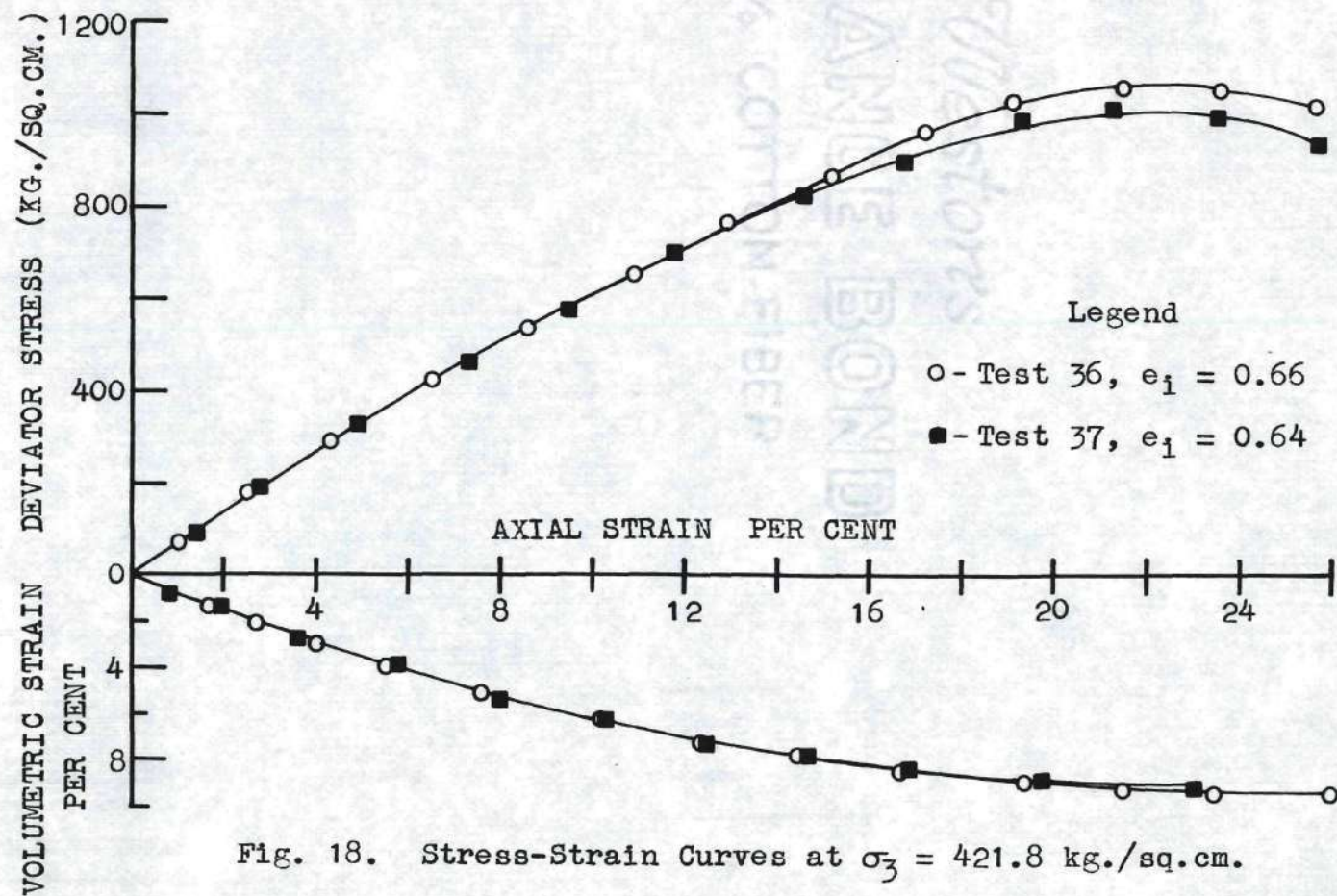


Fig. 18. Stress-Strain Curves at $\sigma_3 = 421.8$ kg./sq.cm.

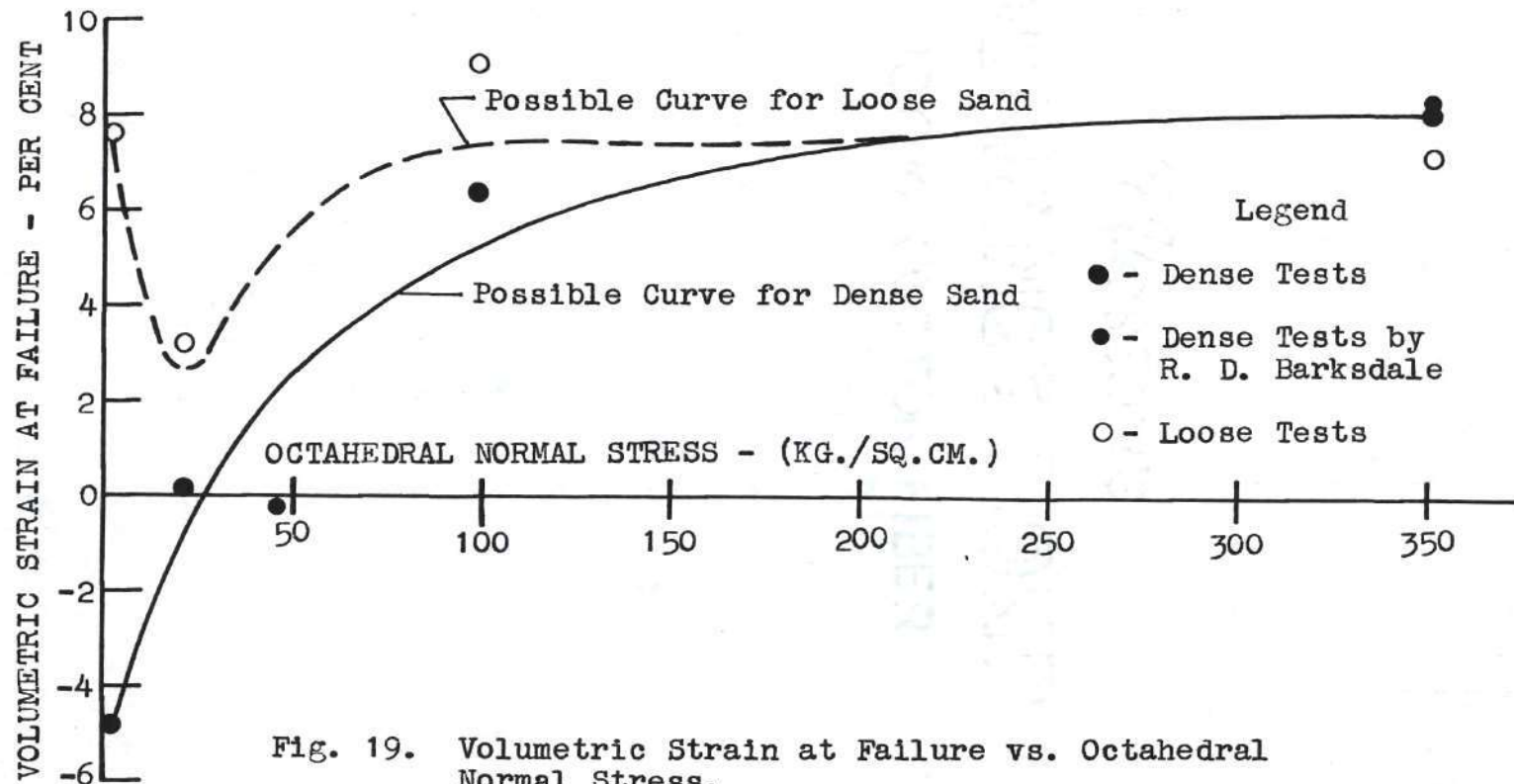


Fig. 19. Volumetric Strain at Failure vs. Octahedral Normal Stress.

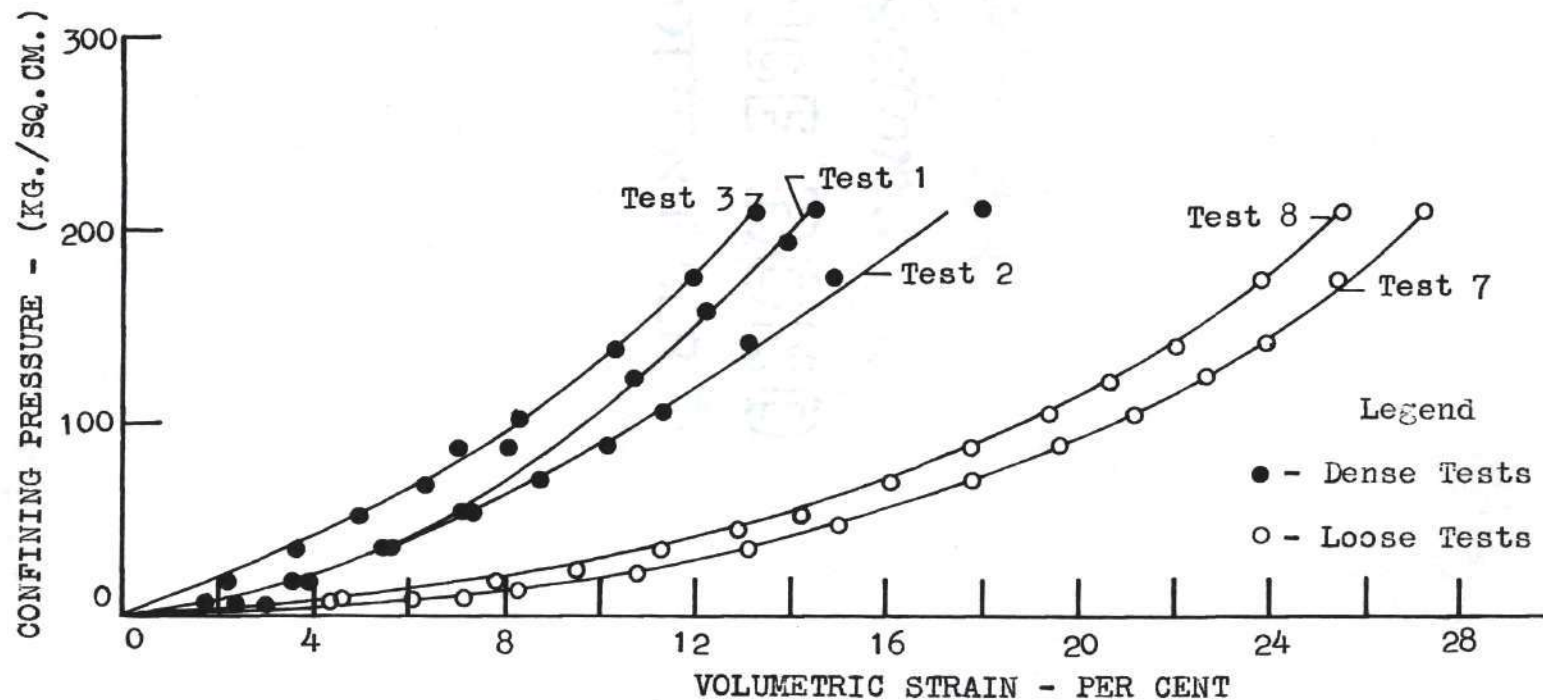


Fig. 20. Confining Pressure vs. Volumetric Strain for Tests 1, 2, 3, 7 and 8.

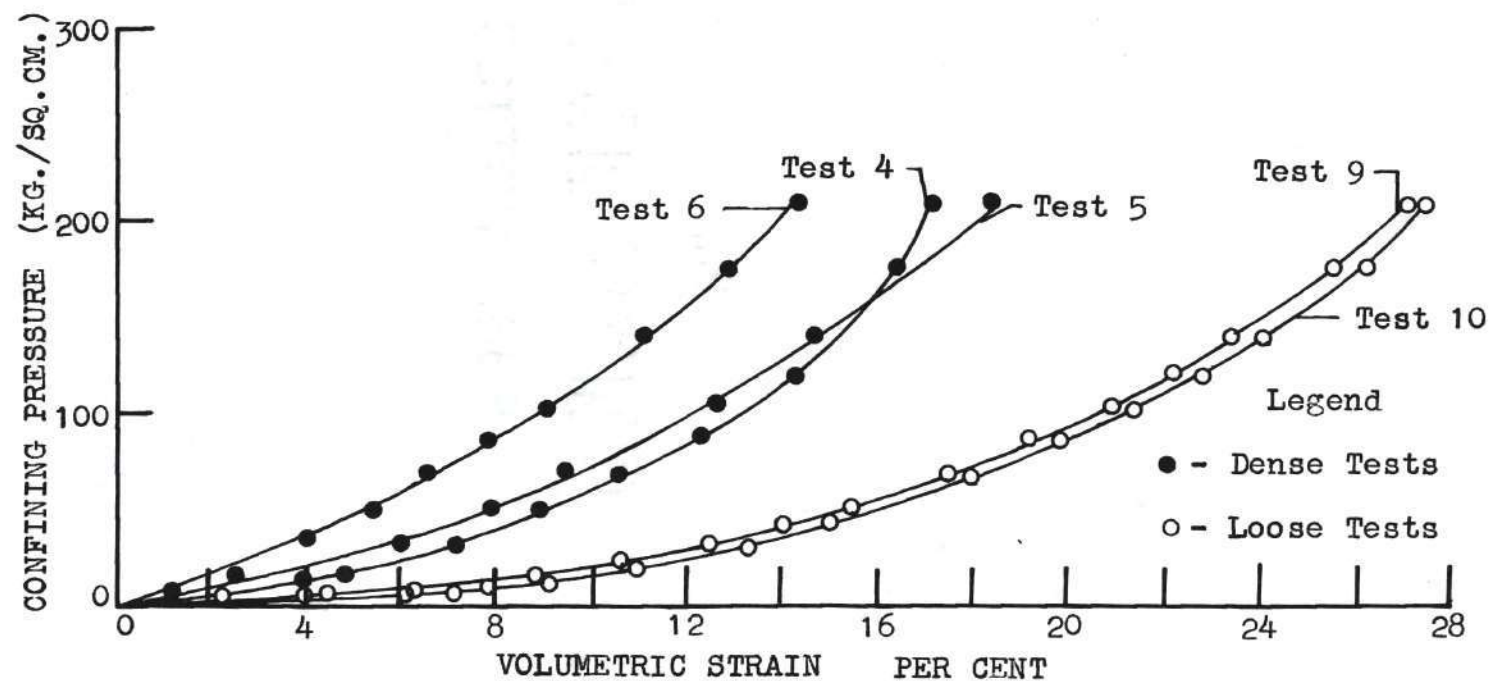


Fig. 21. Confining Pressure vs. Volumetric Strain for Tests 4, 5, 6, 9, and 10.

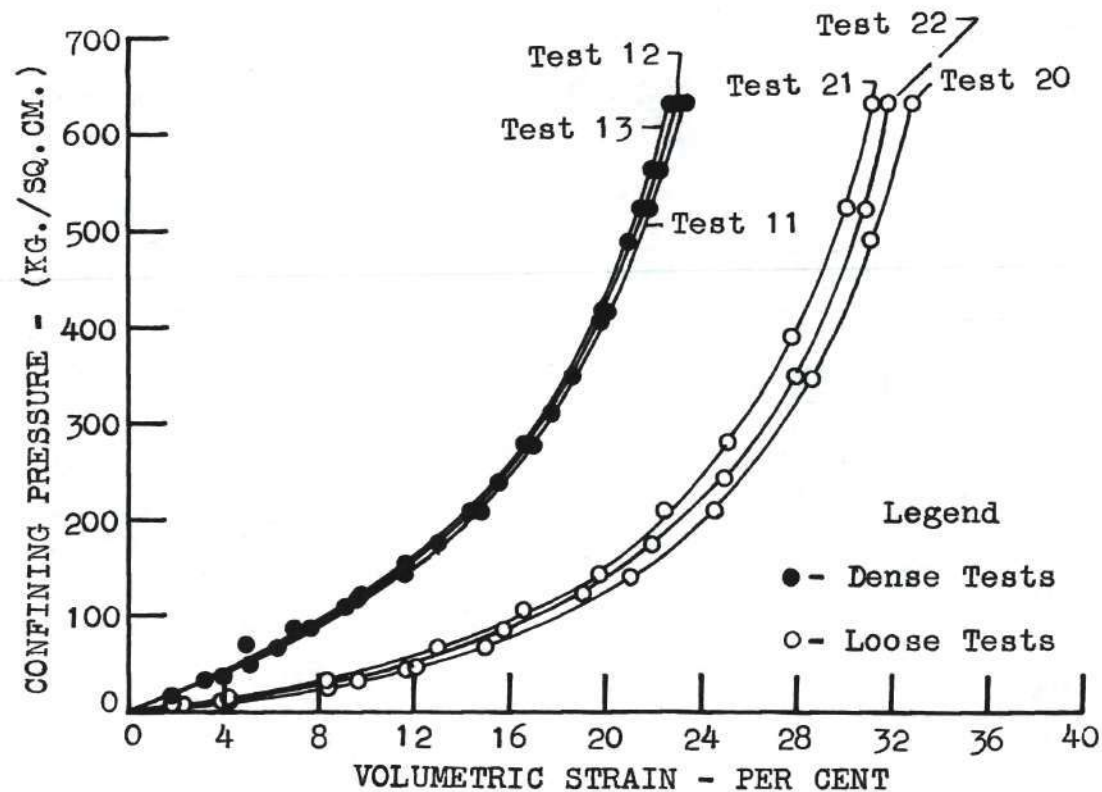


Fig. 22. Confining Pressure vs. Volumetric Strain for Tests 11, 12, 13, 20, 21 and 22.

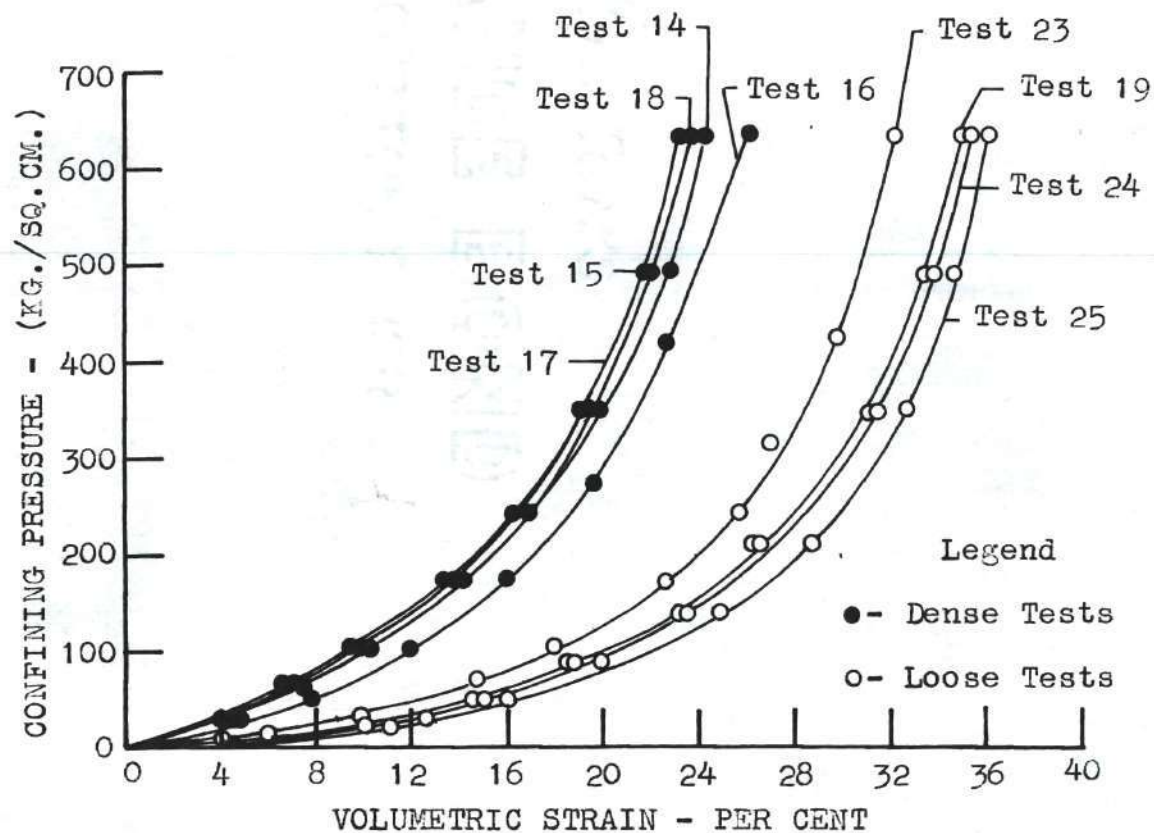


Fig. 23. Confining Pressure vs. Volumetric Strain for Tests 14, 15, 16, 17, 18, 19, 23, 24 and 25.

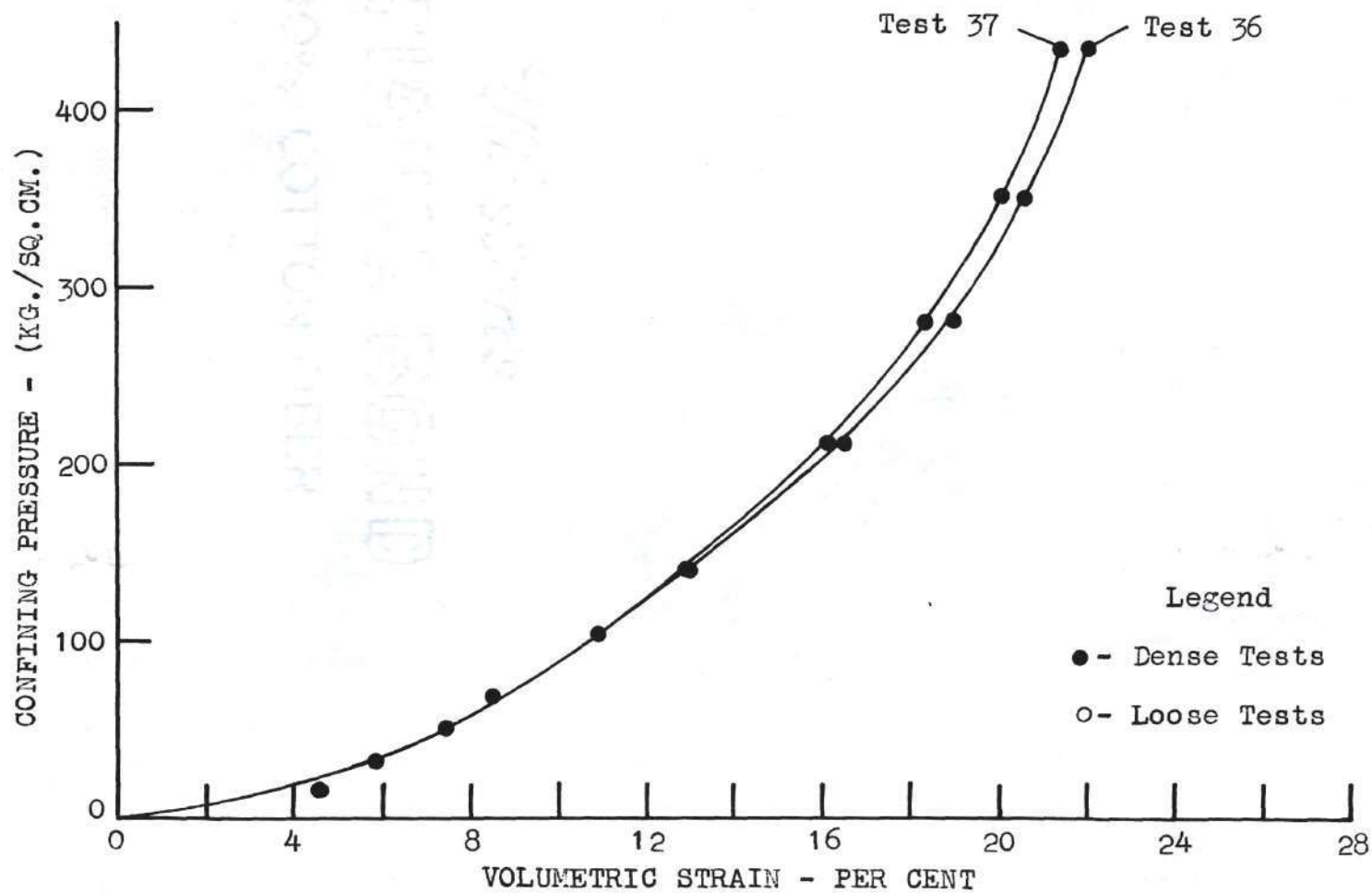


Fig. 24. Confining Pressure vs. Volumetric Strain for Tests 36 and 37.

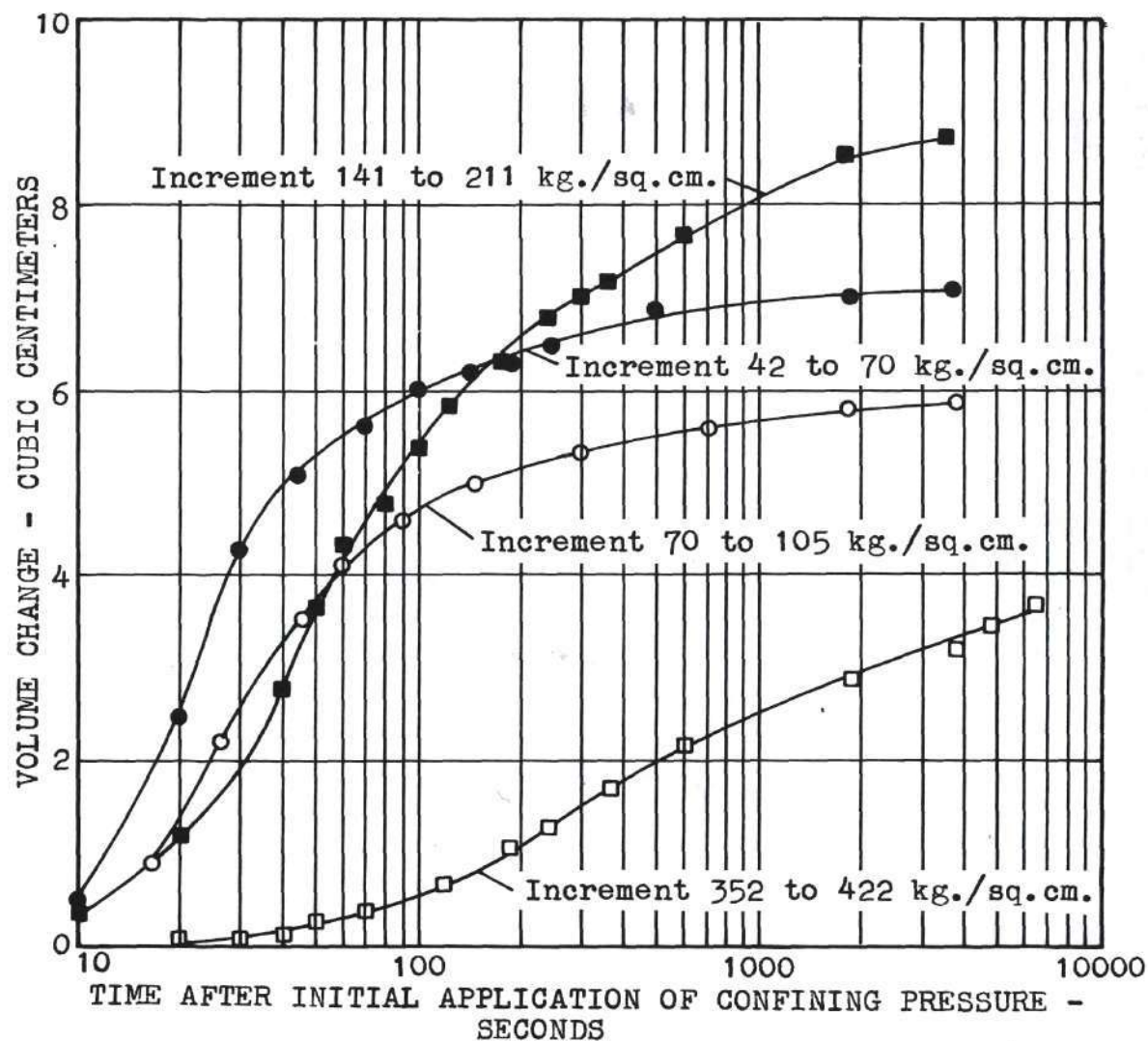


Fig. 25. Volume Change vs. Time after Initial Application of Confining Pressure.

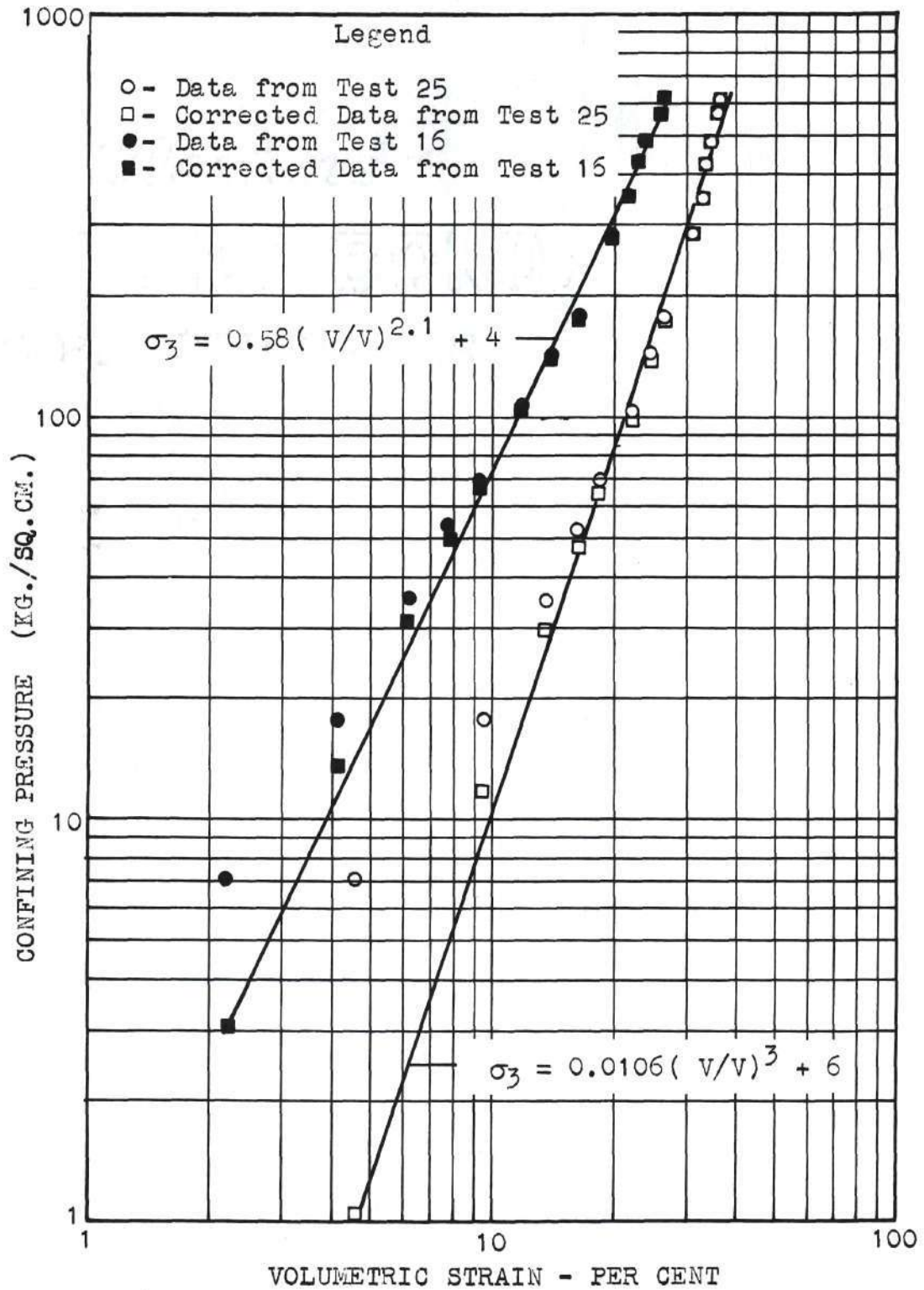
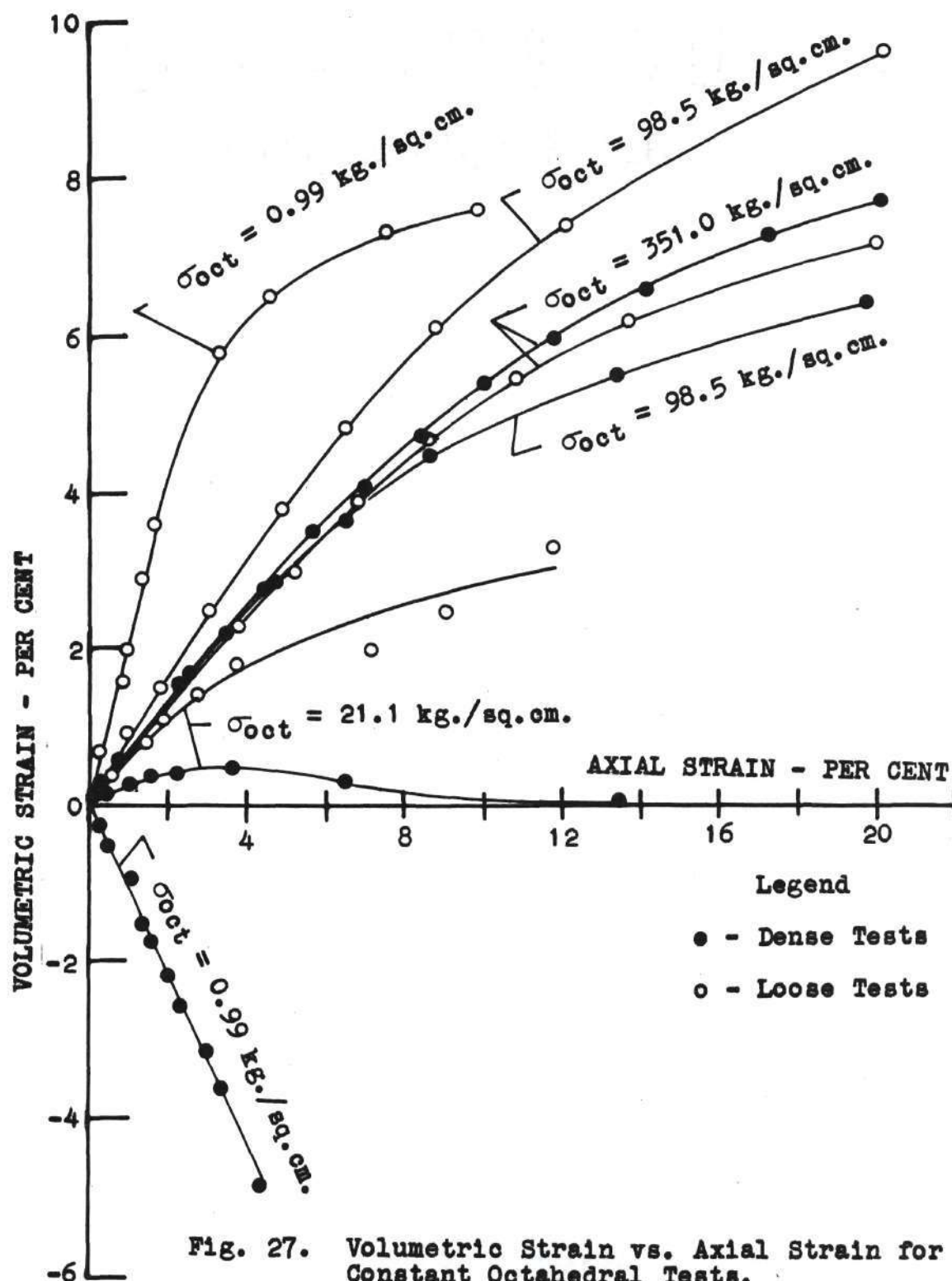


Fig. 26. Logarithm of Confining Pressure vs. Logarithm of Volumetric Strain for Tests 16 and 25.



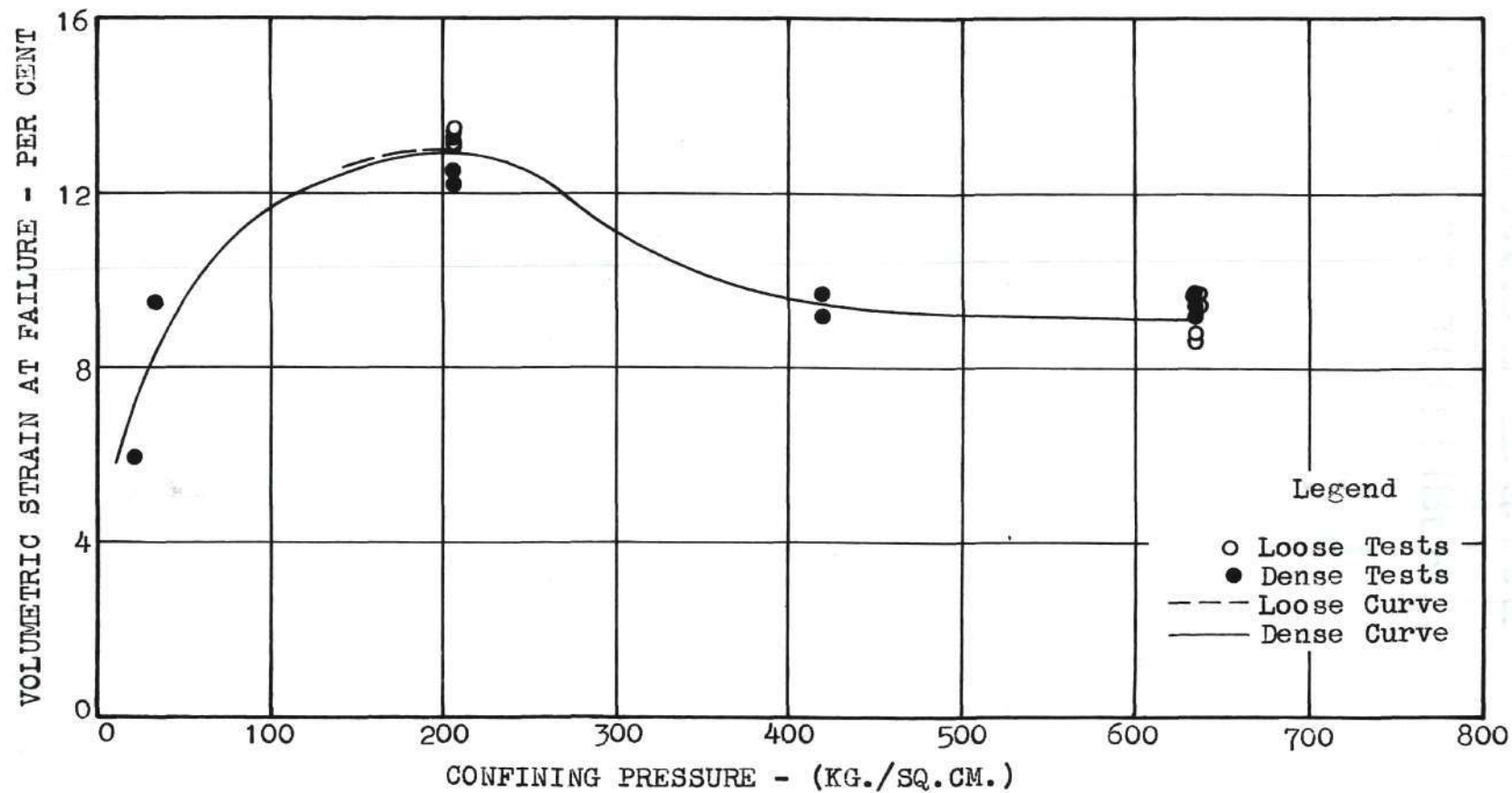


Fig. 28. Volumetric Strain at Failure vs. Confining Pressure

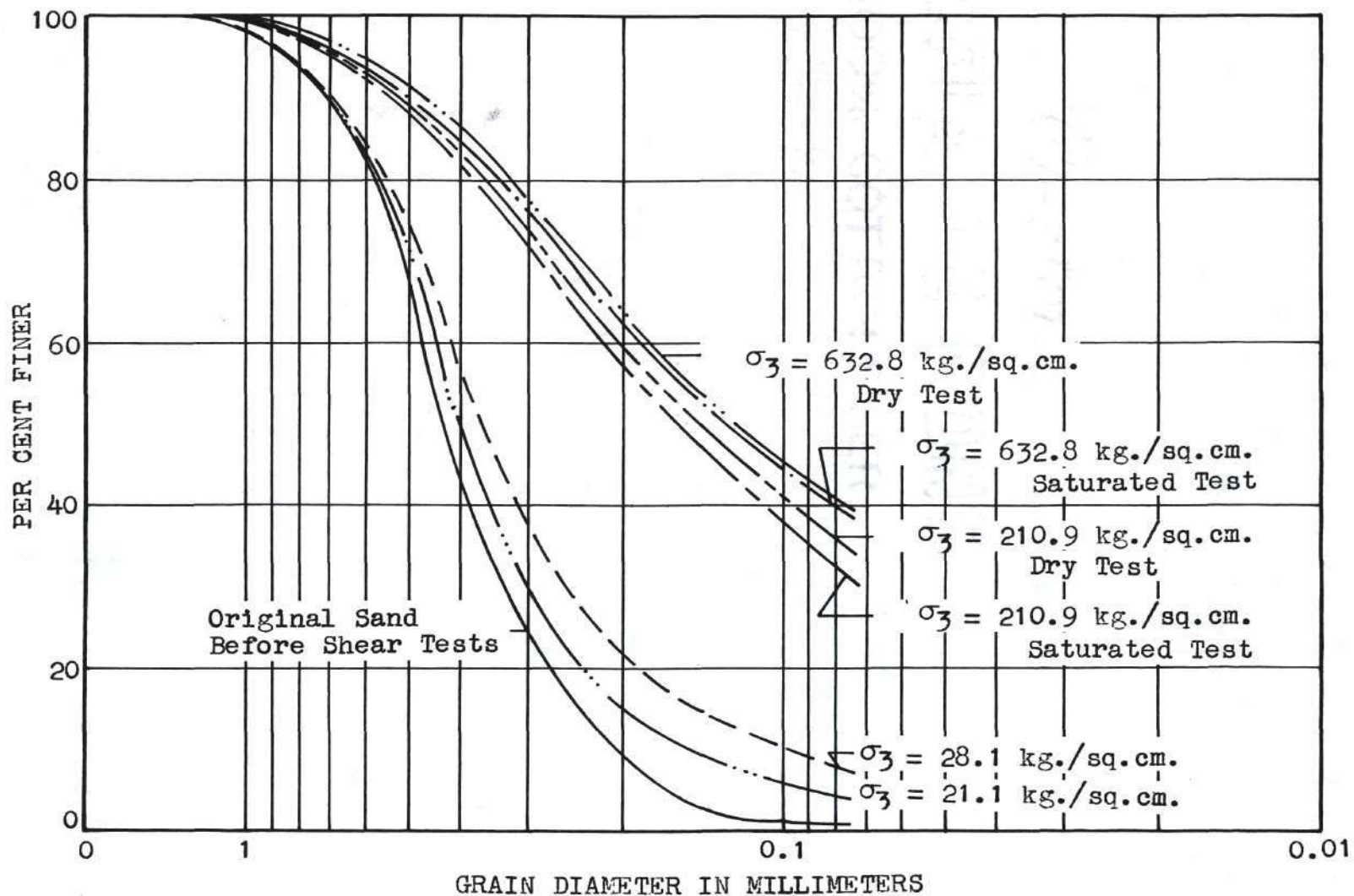


Fig. 29. Grain Size Curves for Various Stages of Confining Pressure.

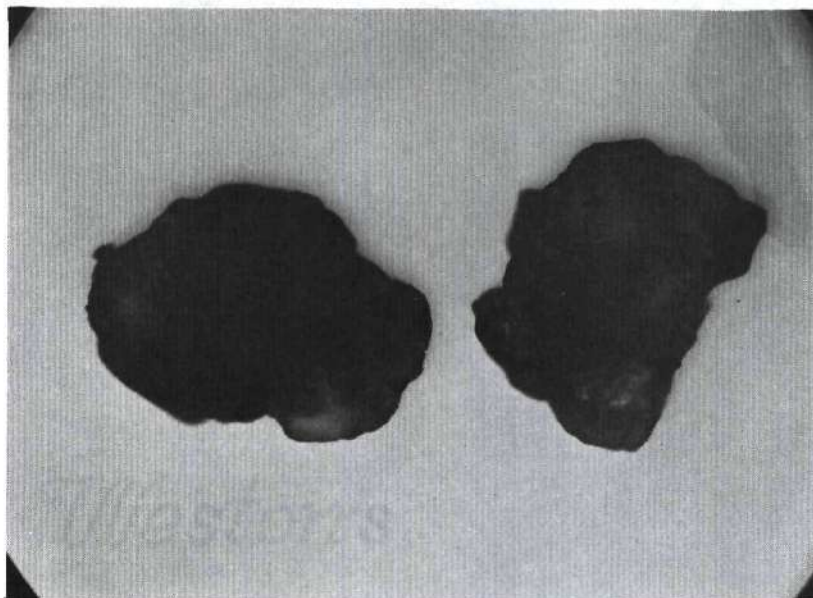


Figure 30. Optical Micrograph of Original Sand Magnified 70 Times.

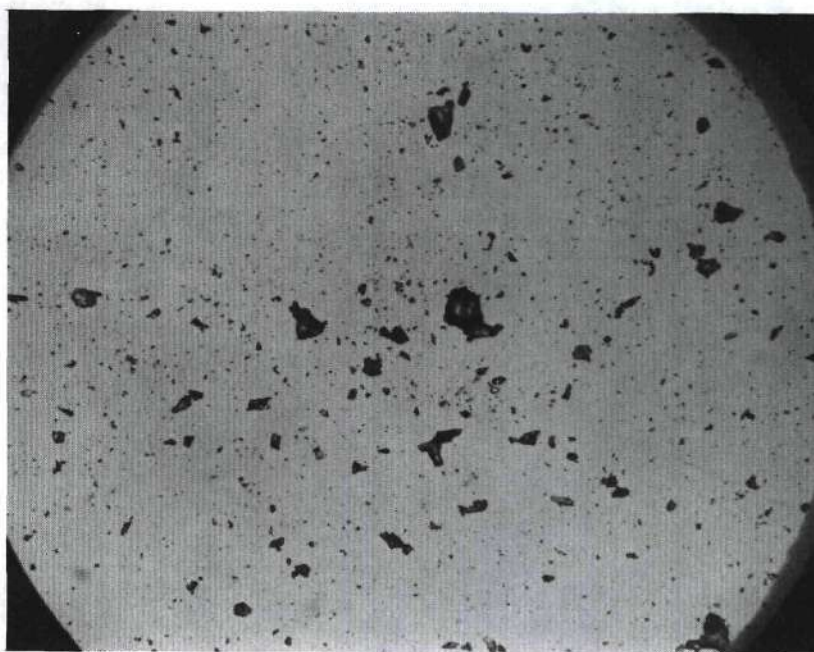


Fig. 31. Optical Micrograph of Sand Confined and Sheared at 632.8 kg./sq.cm. Magnified 70 Times.

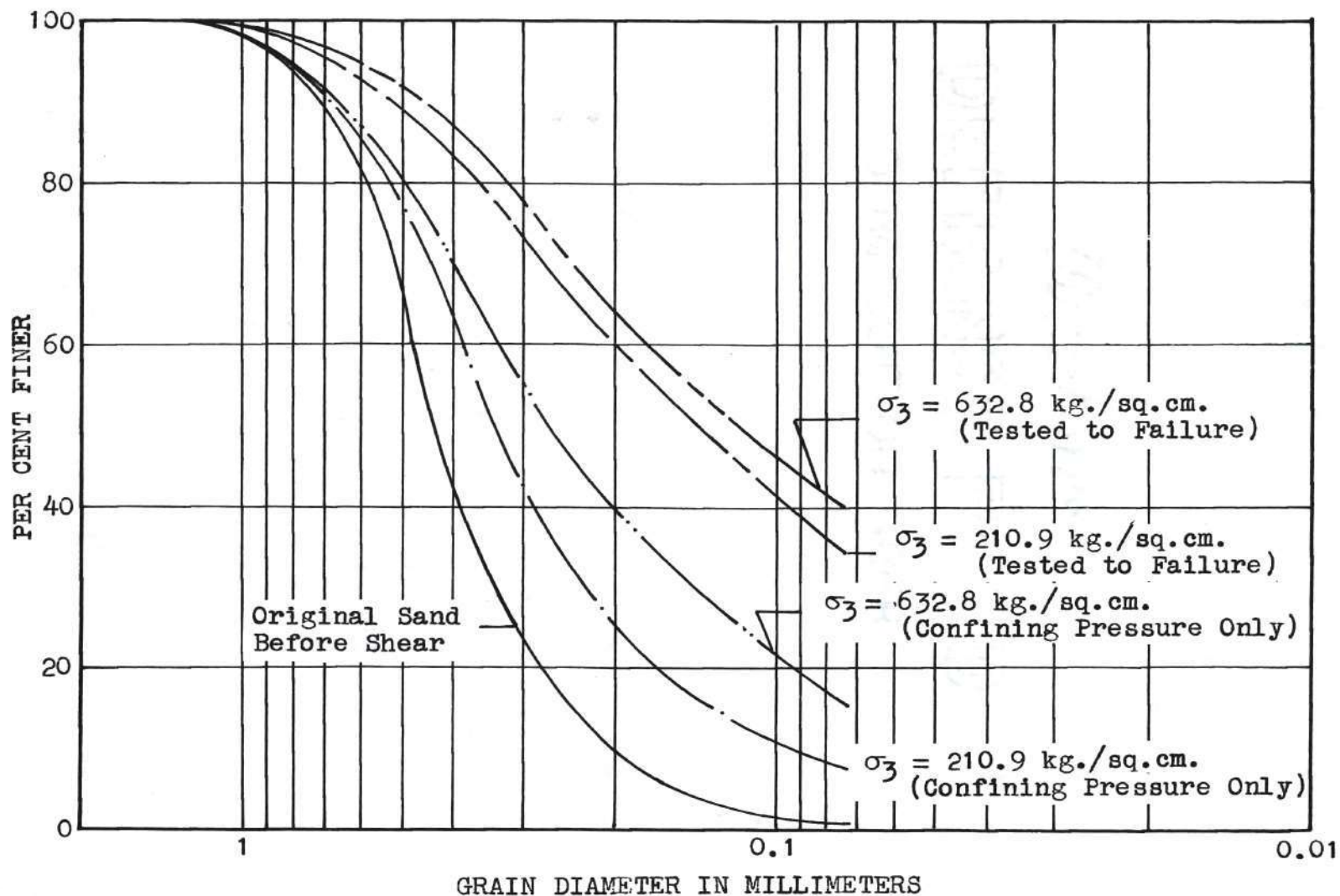


Fig. 32. Grain Size Curves Contrasting Sheared Samples and Isotropically Confined Samples.

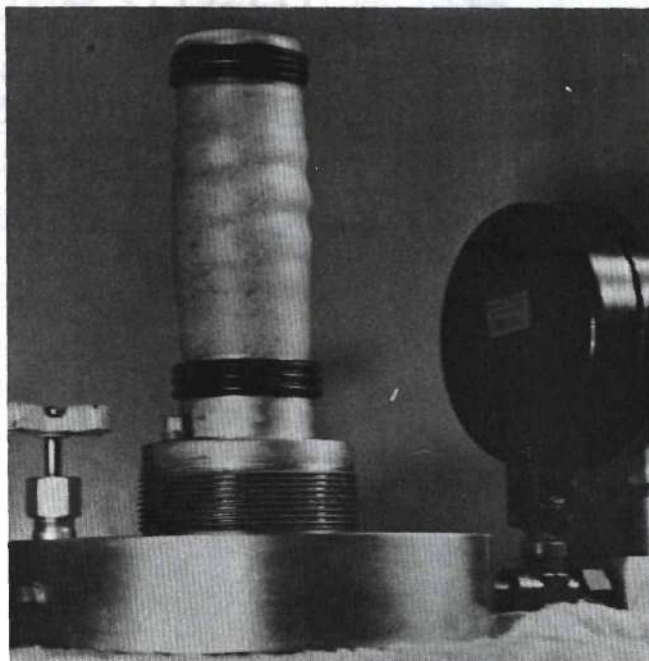


Fig. 33. Bulging Failure at 210.9 kg./sq.cm.

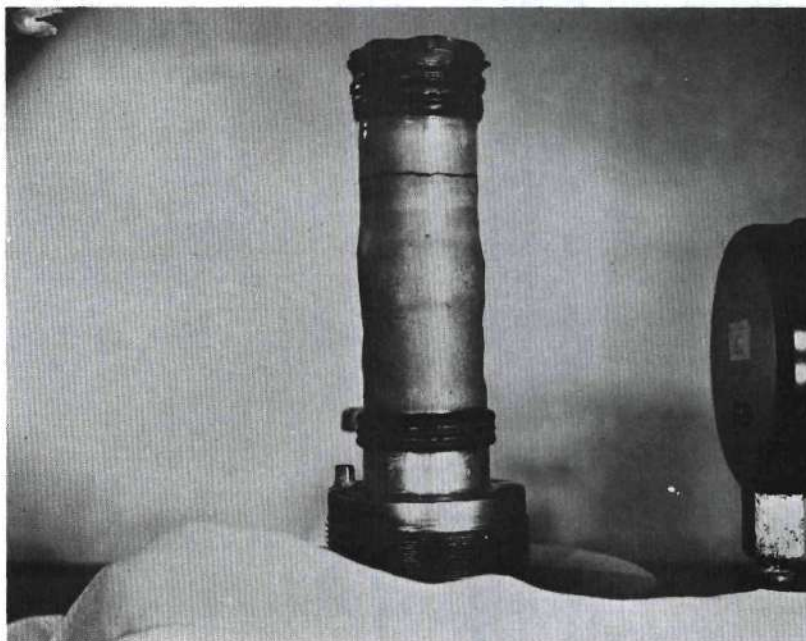


Fig. 34. Bulging Failure at 632.8 kg./sq.cm.

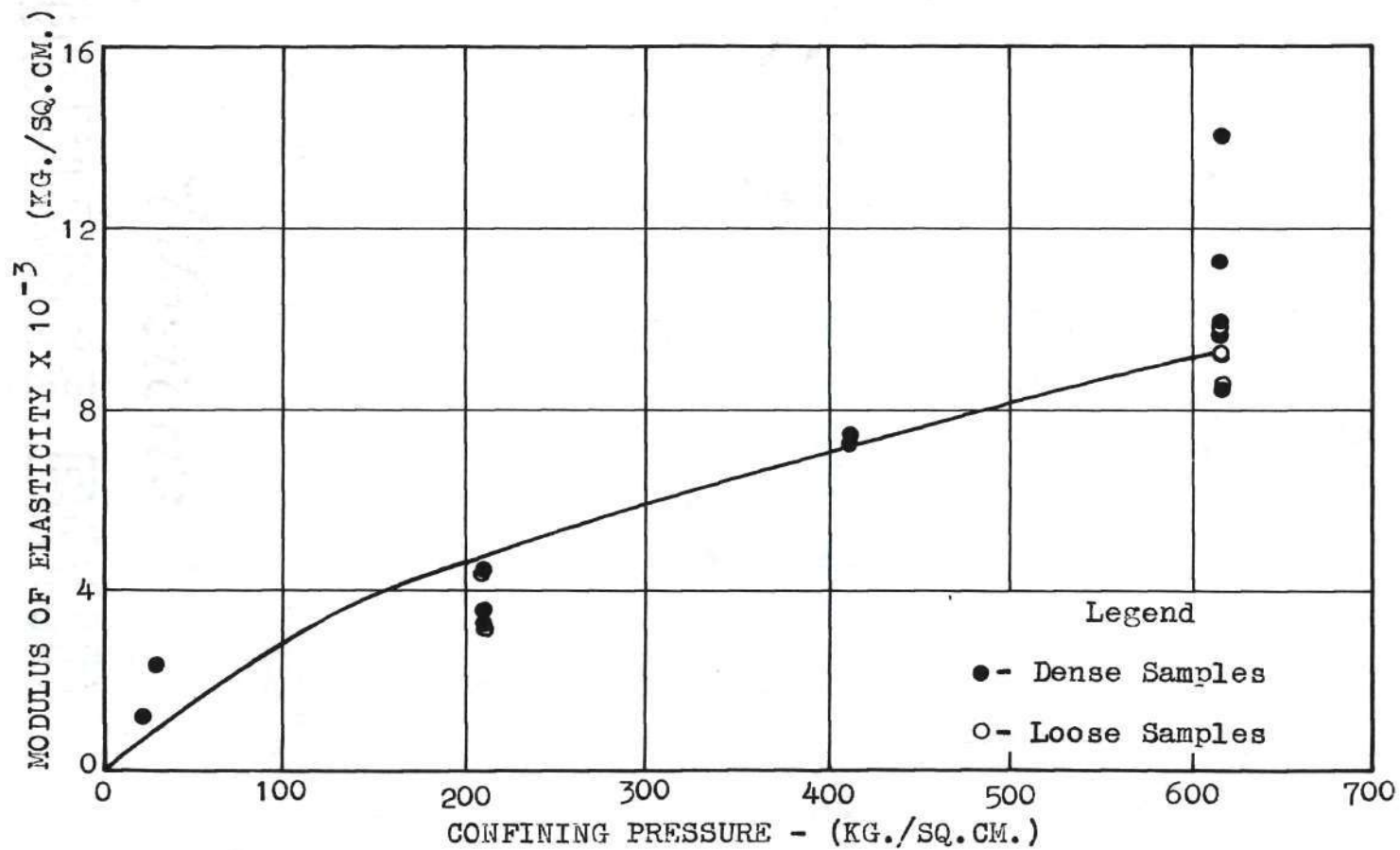


Fig. 35. Initial Tangent Modulus vs. Confining Pressure

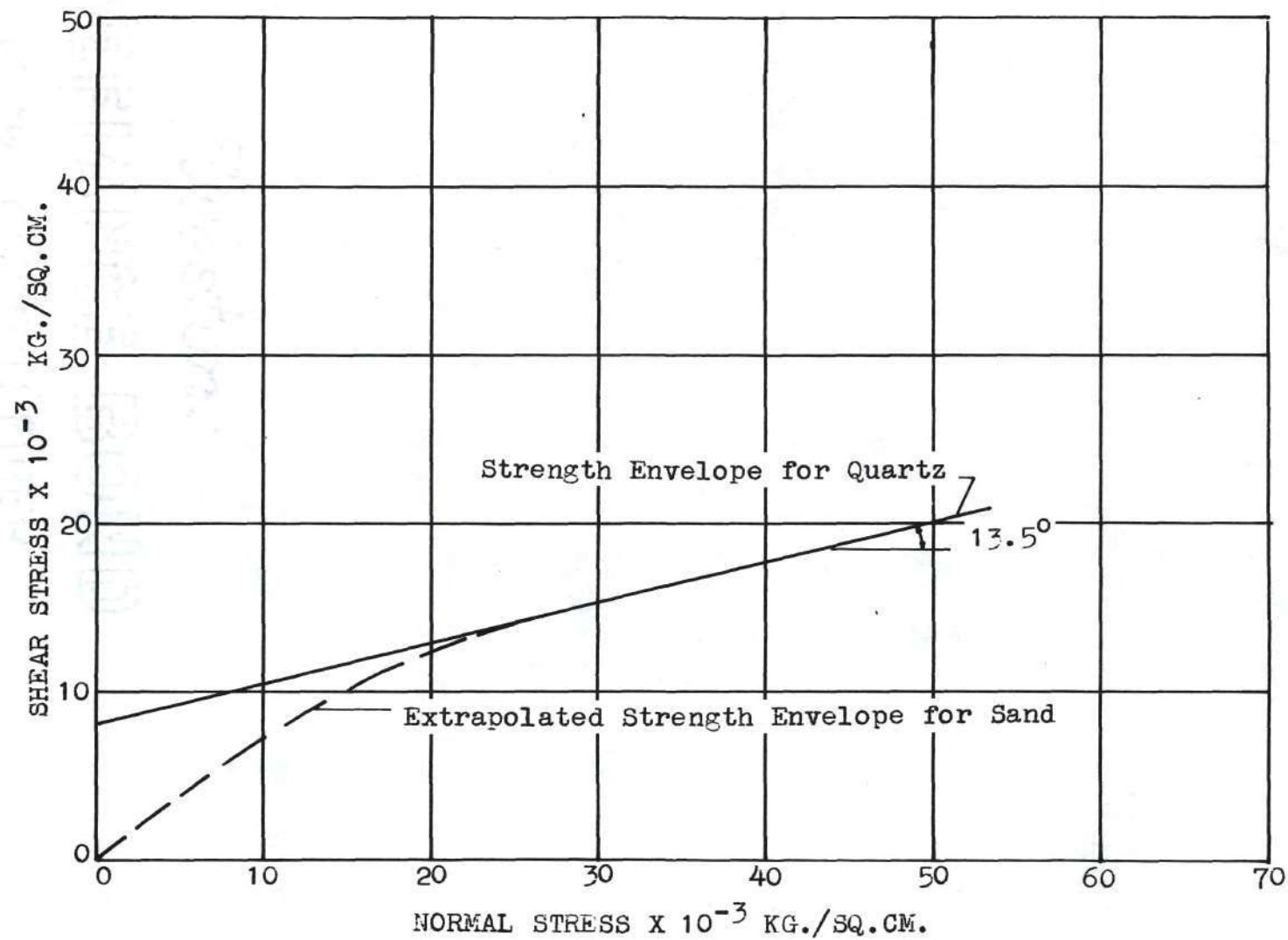


Fig. 36. Extrapolated Sand Envelope to Meet Quartz Envelope.

BIBLIOGRAPHY

LITERATURE CITED

1. A. S. Vesić, *Theoretical studies of Cratering Mechanisms Affecting the Stability of Cratered Slopes*, Soil Mechanics Laboratory, Georgia Institute of Technology, 1963.
2. T. Von Kármán, "Festigkeitsversuche unter allseitigem Druck," *Zeitschrift des Vereines deutscher Ingenieure*, Vol. 55, No. 42, 1911, pp. 1749-1757.
3. P. W. Bridgman, "Recent Work in the Field of High Pressures," *Reviews of Modern Physics*, 1946, Vol. 18, pp. 46-49.
4. D. T. Griggs, "Deformation of Rocks under High Confining Pressures," *The Journal of Geology*, Vol. 44, 1936, pp. 541-577.
5. R. F. Blanks and D. McHenry, "Large Triaxial Testing Machine Built by the Bureau of Reclamation," *Engineering News Record*, Vol. 171, 1945, pp. 113-115.
6. K. Terzaghi and R. B. Peck, *Soil Mechanics in Engineering Practice*, John Wiley and Sons, Inc., London, 1948, p. 58.
7. B. Ladanyi, "Etude des Relations Entre Les Contraintes Et Les Deformations Lors Du Cisaillement Des Sols Pulverulents," *Annales Des Travaux Publics De Belgique*, 1961, p. 123.
8. E. E. De Beer, "The Scale Effect in Transposition of the Results of Deep-Sounding Tests on the Ultimate Bearing Capacity of Piles and Caisson Foundations," *Geotechnique* 13, 1963, pp. 48-57.
9. R. C. Hirschfield and S. J. Poulos, "High-Pressure Triaxial Tests on a Compacted Sand and an Undisturbed Silt," *Symposium on Laboratory Shear Testing of Soils*, Ottawa, Canada, 1963.
10. P. W. Rowe, "The Stress-Dilatancy Relation for Static Equilibrium of an Assembly of Particles in Contact," *Proceedings Royal Society, Series A*, London, Vol. 269, No. 1339, 1962, p. 504.
11. A. B. Vesić and R. D. Barksdale, "Discussion on Shear Strength of Sand at Very High Pressures," *Symposium on Laboratory Shear Testing of Soils*, Ottawa, Canada, 1963.
12. R. D. Barksdale, *Triaxial Shear Strength of Sand*, Unpublished Special Report, School of Civil Engineering, Georgia Institute of Technology, 1963, p. 15.

13. A. B. Vesić, "Bearing Capacity of Deep Foundations in Sand," 42nd Annual Meeting of the Highway Research Board, Washington, D. C., 1963.
14. A. W. Bishop and D. J. Henkel, *The Measurement of Soil Properties in the Triaxial Test*, Edward Arnold, London, 1957, pp. 70-71.
15. A. E. Schwartz, *An Investigation of the Strength of Rock*, Unpublished Ph. D. Thesis, School of Civil Engineering, Georgia Institute of Technology, 1963, pp. 21-24.
16. D. W. Taylor, *Fundamentals of Soil Mechanics*, John Wiley and Sons, New York, 1948, p. 345.
17. S. Timoshenko and J. N. Goodier, *Theory of Elasticity*, McGraw-Hill Book Company, Inc., New York, 1951, pp. 6-10.
18. A. W. Skempton, "Effective Stress in Soils, Concrete and Rocks," *Proceedings of the Conference on Pore Pressure and Suction in Soils*, Butterworths, London, 1961, p. 7.